Simulations of Idealized Solid Electrolytes*

Natalie A. W. Holzwarth
Department of Physics, Wake Forest University
Winston-Salem, NC. 27109 USA

*Research performed in collaboration with Nicholas Lepley (WFU Ph. D. Dec. 2015), Larry Rush Jr. (WFU MS May 2017), Jason Howard, and Ahmad Al-Qawasmeh (WFU graduate students), Yaojun Du (former WFU Postdoc) and in consultation with Zachary Hood from ORNL and Ga Tech. Collaborations with WFU Chemistry Colleagues --Dr. Keerthi Senevirathne (now at Florida A & M U.), Dr. Cynthia Day, Professor Michael Gross, and Professor Abdessadek Lachgar, are also gratefully acknowledged. Research was supported by NSF grant DMR 1507942 and computations were performed on WFU's DEAC cluster.

Outline

- Motivation – Why solid electrolytes?
- Computational tools & reality checks; what can be learned from "first principles" calculations?
- Simulations of bulk properties and ion mobility
  - Li phosphorus oxynitrides (first developed at Oak Ridge National Laboratory)
  - Li thiophosphates
- Simulations of interfaces with metallic Li
- Summary and remaining challenges

Materials components of a Li or Na ion battery

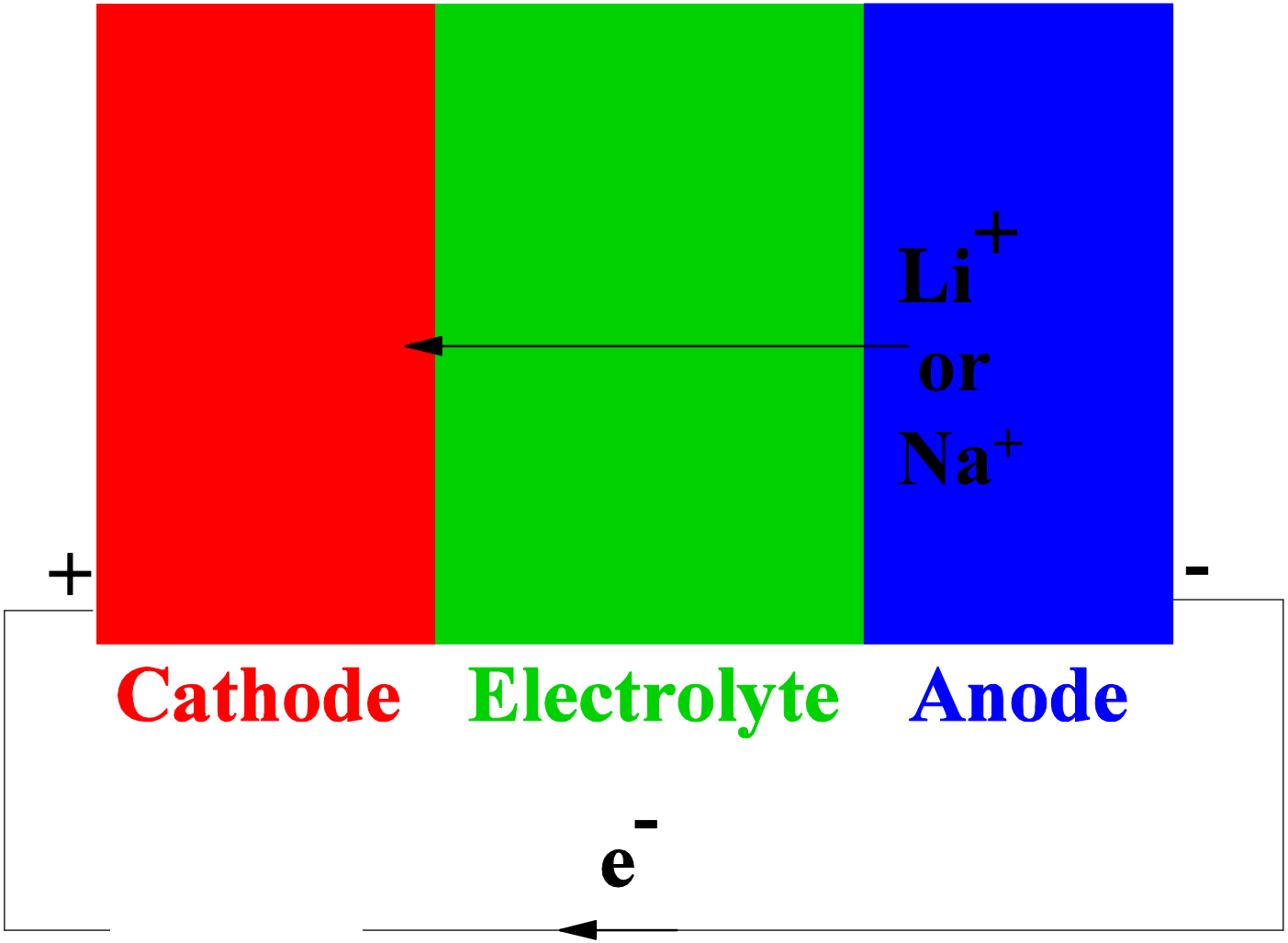

$$V = IR$$

$$\xrightarrow{\quad} I$$

Development of LiPON electrolyte films at Oak Ridge National Laboratory

Solid State Ionics 53–56 (1992) 655–661
North-Holland

WAKE FOREST UNIVERSITY

SOLID STATE IONICS

Sputtering of lithium compounds for preparation of electrolyte thin films

N.J. Dudney, J.B. Bates, R.A. Zuhr and C.F. Luck
Solid State Division, Oak Ridge National Laboratory, P O Box 2008, Oak Ridge, TN 37831-6030, USA

JOURNAL OF SOLID STATE CHEMISTRY **115**, 313–323 (1995)

Synthesis, Crystal Structure, and Ionic Conductivity of a Polycrystalline Lithium Phosphorus Oxynitride with the γ-Li_3PO_4 Structure

B. Wang, B. C. Chakoumakos, B. C. Sales, B. S. Kwak, and J. B. Bates

From Oak Ridge National Laboratory:

Materials Views
www.MaterialsViews.com
Adv. Energy Mater. **2015**, *5*, 1401408
DOI: 10.1002/aenm.201401408
ADVANCED ENERGY MATERIALS
www.advenergymat.de

Solid Electrolyte: the Key for High-Voltage Lithium Batteries

Juchuan Li, Cheng Ma, Miaofang Chi, Chengdu Liang, and Nancy J. Dudney**

Advantages

- **Compatible and stable with high voltage cathodes and with Li metal anodes**

Disadvantages

- **Relatively low ionic conductivity (Compensated with the use of less electrolyte?)**
- **Lower total capacity**

Demonstrated for $LiNi_{0.5}Mn_{1.5}O_4$/LiPON/Li

- **10^{-6} m LiPON electrolyte layer achieved adequate conductivity**
- **10,000 cycles* with 90% capacity retention**

***1 cycle per day for 27 years**

Motivation: Paper by N. Kayama, *et. al* in ***Nature Materials* 10**, 682-686 (2011)

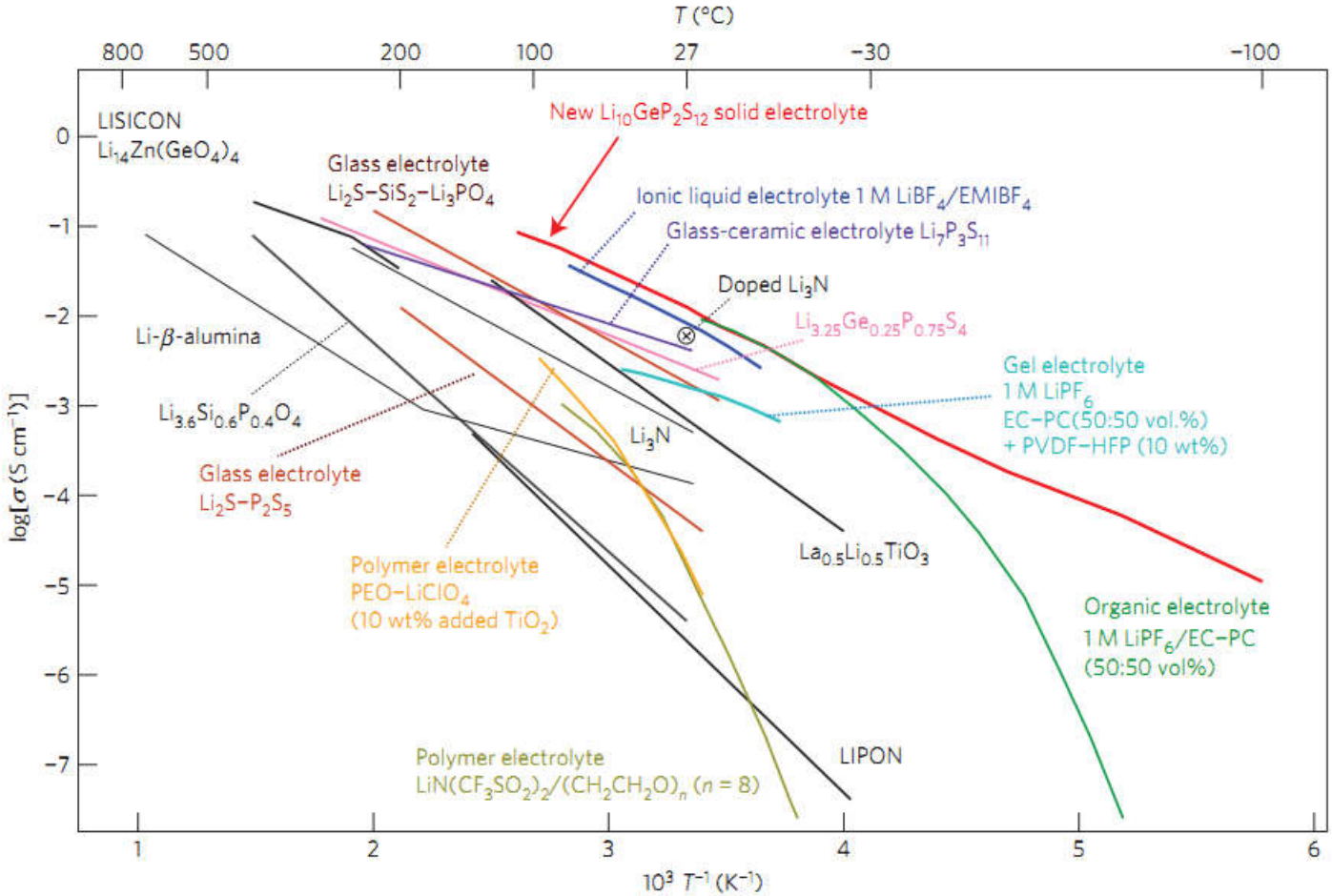

Figure 3 | Thermal evolution of ionic conductivity of the new $Li_{10}GeP_2S_{12}$ phase, together with those of other lithium solid electrolytes, organic liquid electrolytes, polymer electrolytes, ionic liquids and gel electrolytes[3-8,13-16,20,22]**.** The new $Li_{10}GeP_2S_{12}$ exhibits the highest lithium ionic conductivity (12 m S cm^{-1} at 27 °C) of the solid lithium conducting membranes of inorganic, polymer or composite systems. Because organic electrolytes usually have transport numbers below 0.5, inorganic lithium electrolytes have extremely high conductivities.

Motivation: Paper by N. Kamaya, *et. al* in ***Nature Materials*** **10**, 682-686 (2011)

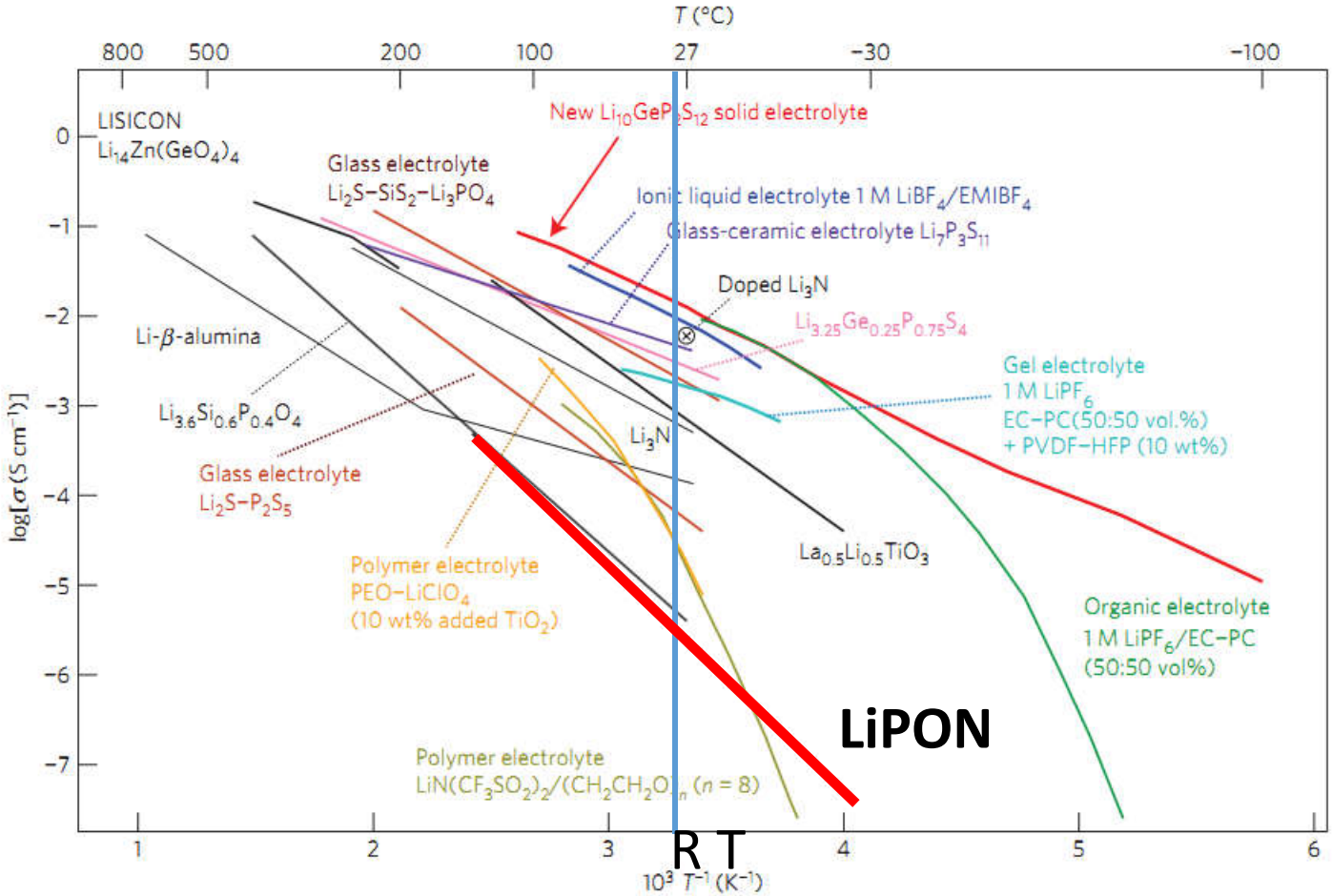

Figure 3 | Thermal evolution of ionic conductivity of the new $Li_{10}GeP_2S_{12}$ phase, together with those of other lithium solid electrolytes, organic liquid electrolytes, polymer electrolytes, ionic liquids and gel electrolytes[3-8,13-16,20,22]**.** The new $Li_{10}GeP_2S_{12}$ exhibits the highest lithium ionic conductivity (12 m S cm^{-1} at 27 °C) of the solid lithium conducting membranes of inorganic, polymer or composite systems. Because organic electrolytes usually have transport numbers below 0.5, inorganic lithium electrolytes have extremely high conductivities.

Motivation: Paper by N. Kamaya, *et. al* in ***Nature Materials*** **10**, 682-686 (2011)

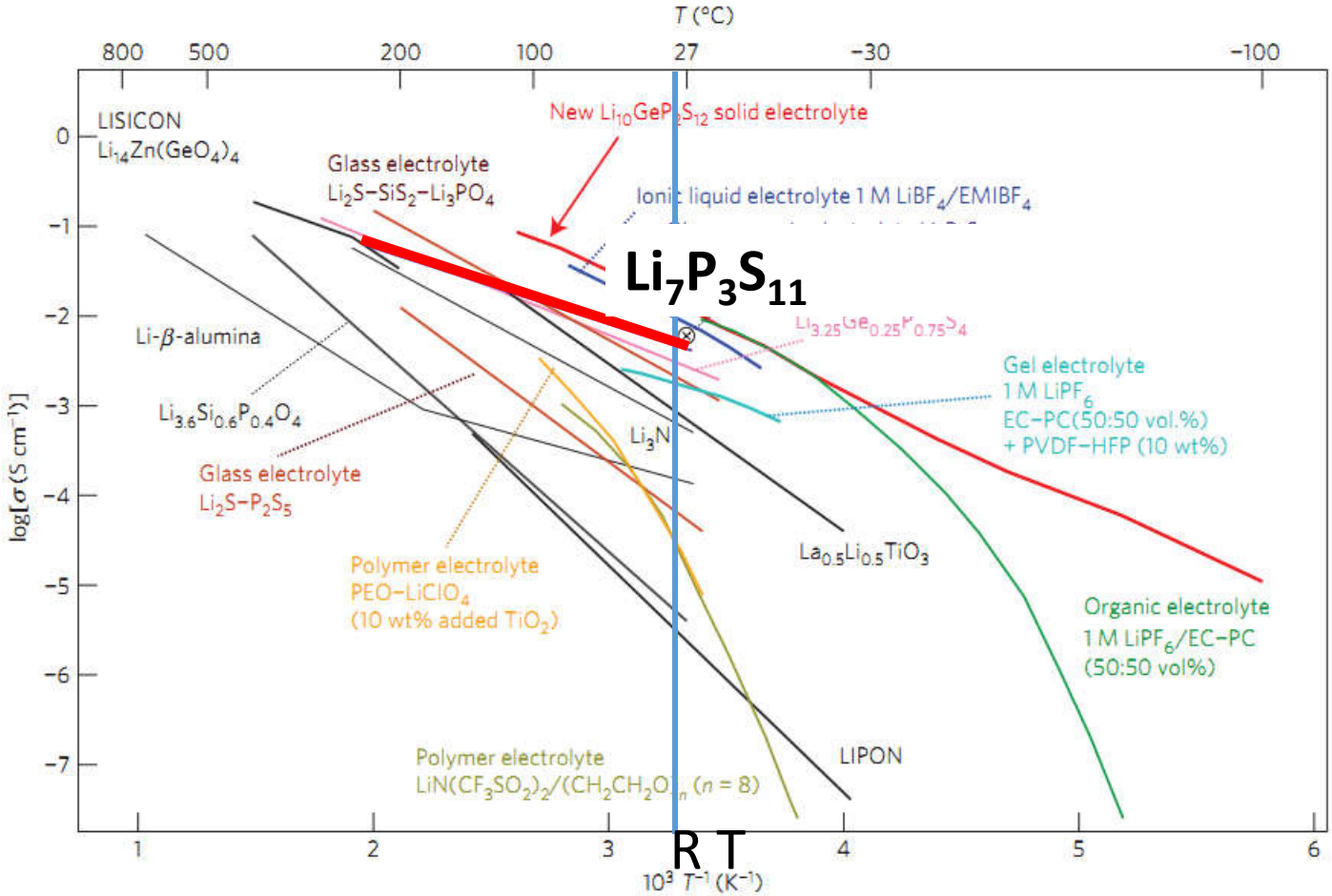

Figure 3 | Thermal evolution of ionic conductivity of the new $Li_{10}GeP_2S_{12}$ phase, together with those of other lithium solid electrolytes, organic liquid electrolytes, polymer electrolytes, ionic liquids and gel electrolytes[3-8,13-16,20,22]**.** The new $Li_{10}GeP_2S_{12}$ exhibits the highest lithium ionic conductivity (12 m S cm^{-1} at 27 °C) of the solid lithium conducting membranes of inorganic, polymer or composite systems. Because organic electrolytes usually have transport numbers below 0.5, inorganic lithium electrolytes have extremely high conductivities.

Motivation: Paper by N. Kamaya, *et. al* in ***Nature Materials*** **10**, 682-686 (2011)

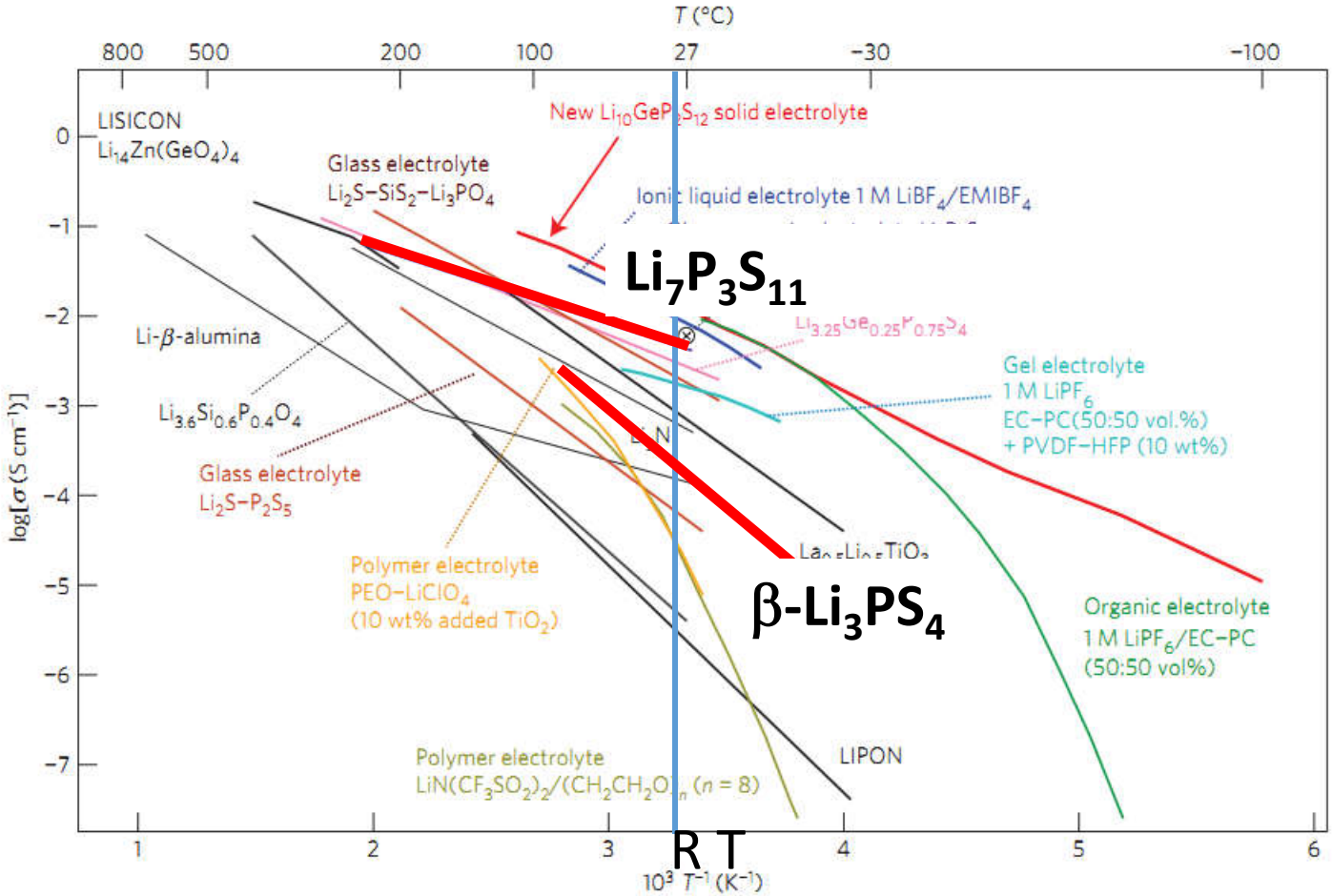

Figure 3 | Thermal evolution of ionic conductivity of the new $Li_{10}GeP_2S_{12}$ phase, together with those of other lithium solid electrolytes, organic liquid electrolytes, polymer electrolytes, ionic liquids and gel electrolytes[3-8,13-16,20,22]**.** The new $Li_{10}GeP_2S_{12}$ exhibits the highest lithium ionic conductivity (12 m S cm^{-1} at 27 °C) of the solid lithium conducting membranes of inorganic, polymer or composite systems. Because organic electrolytes usually have transport numbers below 0.5, inorganic lithium electrolytes have extremely high conductivities.

Motivation: Paper by N. Kamaya, *et. al* in ***Nature Materials*** **10**, 682-686 (2011)

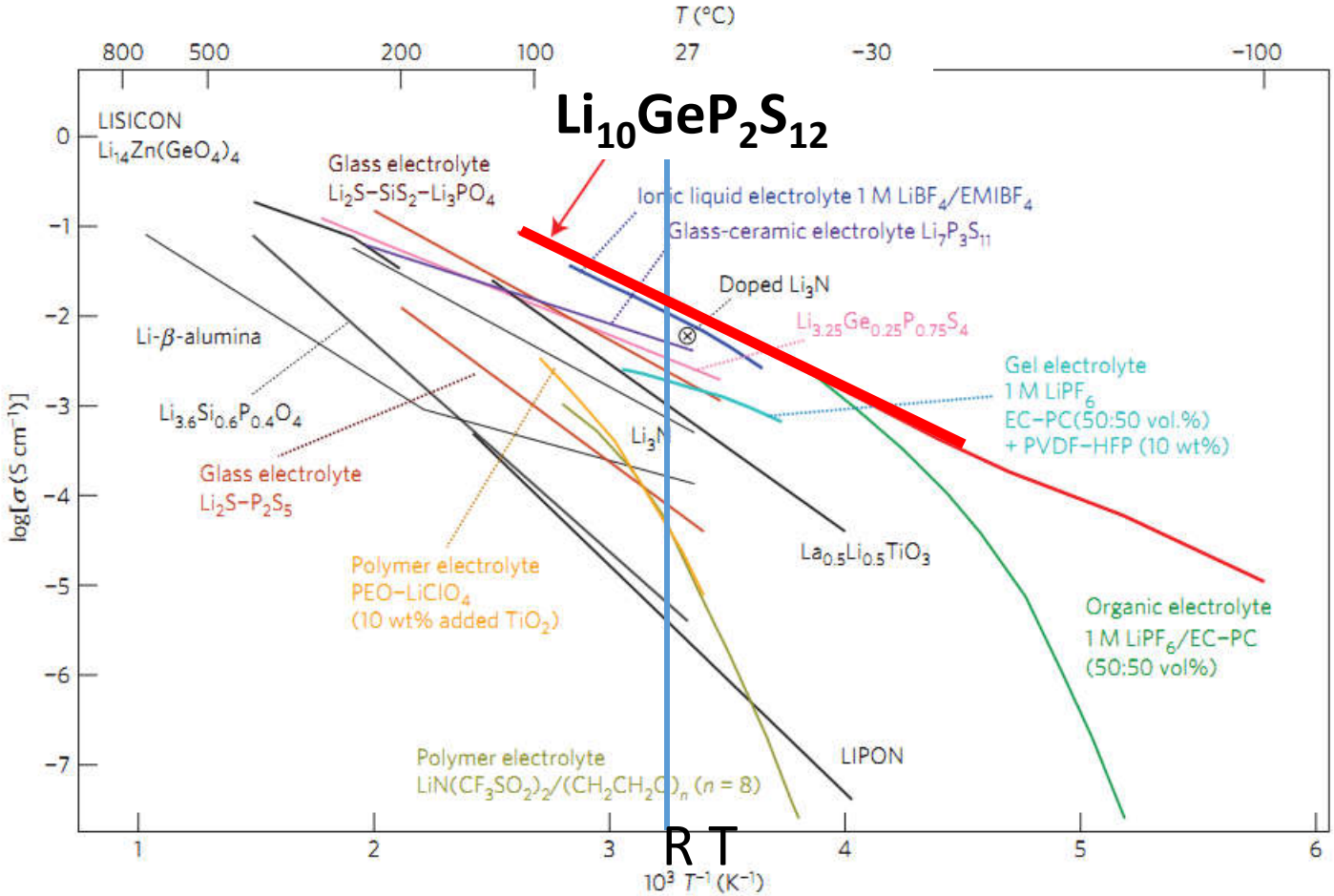

Figure 3 | Thermal evolution of ionic conductivity of the new $Li_{10}GeP_2S_{12}$ phase, together with those of other lithium solid electrolytes, organic liquid electrolytes, polymer electrolytes, ionic liquids and gel electrolytes[3-8,13-16,20,22]**.** The new $Li_{10}GeP_2S_{12}$ exhibits the highest lithium ionic conductivity (12 m S cm^{-1} at 27 °C) of the solid lithium conducting membranes of inorganic, polymer or composite systems. Because organic electrolytes usually have transport numbers below 0.5, inorganic lithium electrolytes have extremely high conductivities.

Solid electrolyte families investigated in this study:

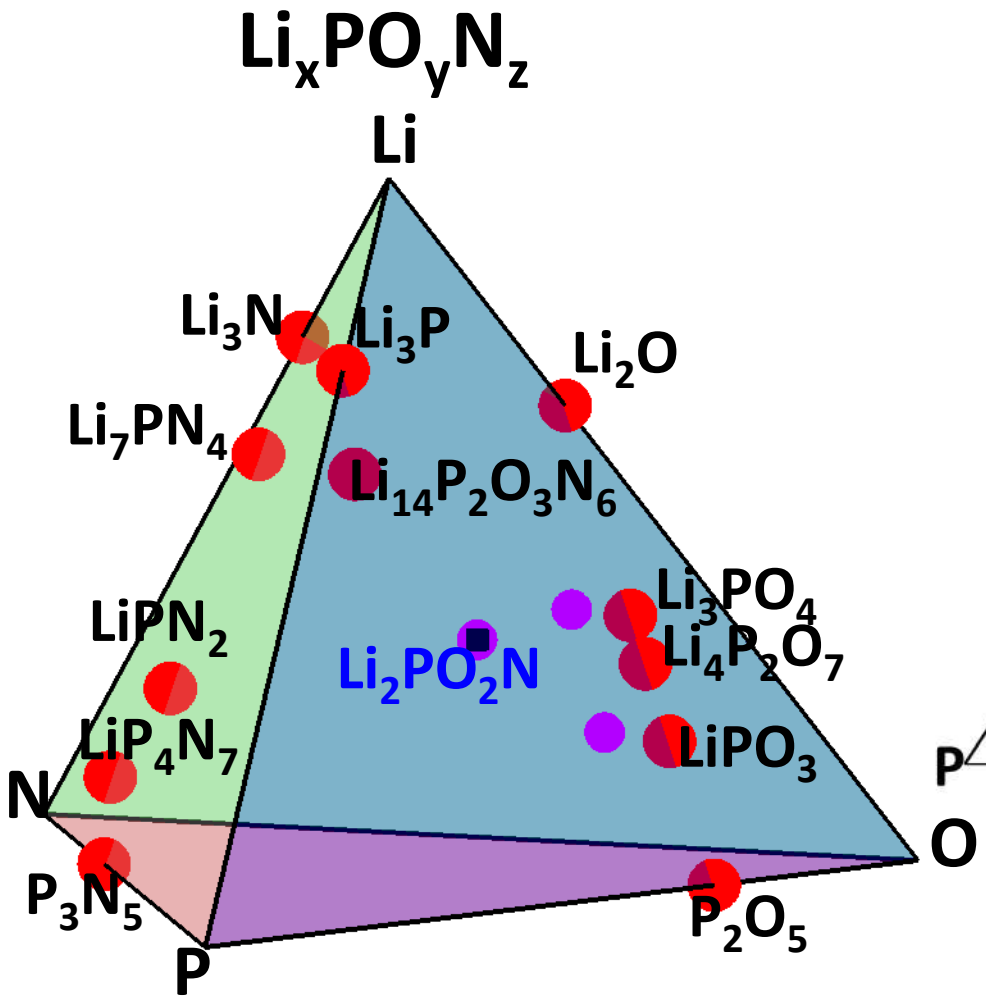

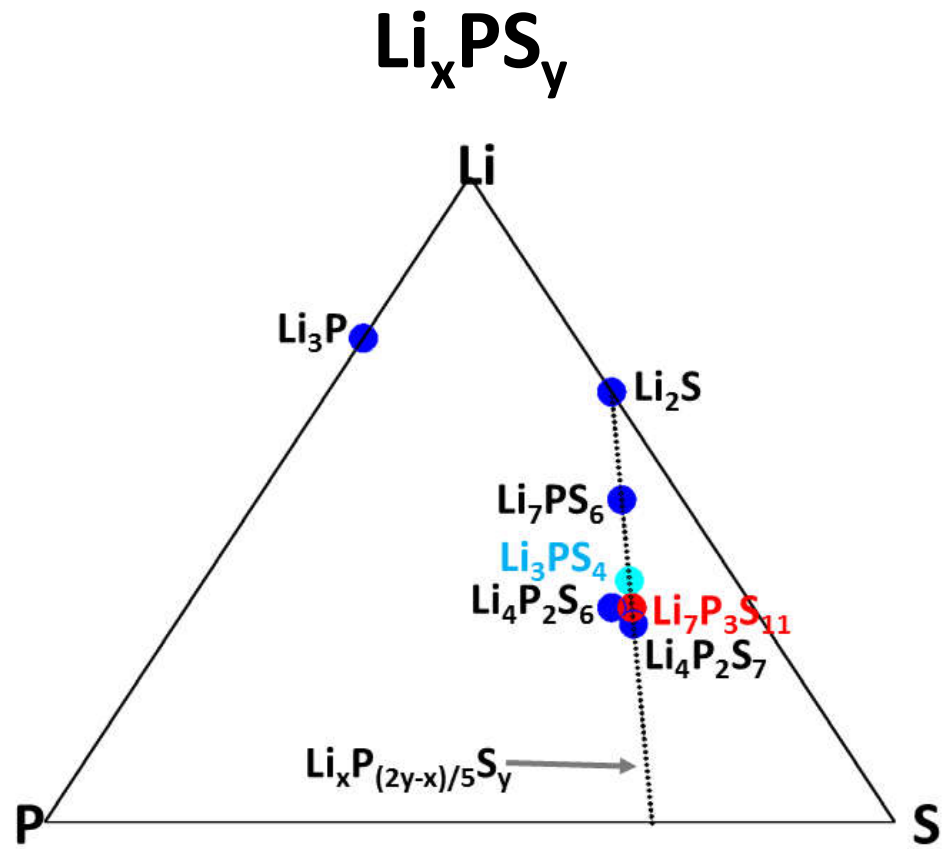

Computational tools

Summary of "first-principles" calculation methods

Electronic coordinates

Atomic coordinates

Exact Schrödinger equation:

$$\mathcal{H}(\{\mathbf{r}_i\},\{\mathbf{R}^a\})\Psi_\alpha(\{\mathbf{r}_i\},\{\mathbf{R}^a\}) = E_\alpha \Psi_\alpha(\{\mathbf{r}_i\},\{\mathbf{R}^a\})$$

where

$$\mathcal{H}(\{\mathbf{r}_i\},\{\mathbf{R}^a\}) = \mathcal{H}^{\text{Nuclei}}(\{\mathbf{R}^a\}) + \mathcal{H}^{\text{Electrons}}(\{\mathbf{r}_i\},\{\mathbf{R}^a\})$$

Born-Oppenheimer approximation

Born & Huang, **Dynamical Theory of Crystal Lattices**, Oxford (1954)

Approximate factorization:

$$\Psi_\alpha(\{\mathbf{r}_i\},\{\mathbf{R}^a\}) = X_\alpha^{\text{Nuclei}}(\{\mathbf{R}^a\})\Upsilon_\alpha^{\text{Electrons}}(\{\mathbf{r}_i\},\{\mathbf{R}^a\})$$

Treated with classical mechanics

Treated with density functional theory

Electronic Schrödinger equation:

$$\mathcal{H}^{\text{Electrons}}(\{\mathbf{r}_i\},\{\mathbf{R}^a\})\Upsilon_\alpha^{\text{Electrons}}(\{\mathbf{r}_i\},\{\mathbf{R}^a\}) = U_\alpha(\{\mathbf{R}^a\})\Upsilon_\alpha^{\text{Electrons}}(\{\mathbf{r}_i\},\{\mathbf{R}^a\})$$

$$\mathcal{H}^{\text{Electrons}}(\{\mathbf{r}_i\},\{\mathbf{R}^a\}) = -\frac{\hbar^2}{2m}\sum_i \nabla_i^2 - \sum_{a,i}\frac{Z^a e^2}{|\mathbf{r}_i - \mathbf{R}^a|} + \sum_{i<j}\frac{e^2}{|\mathbf{r}_i - \mathbf{r}_j|}$$

For electronic ground state: $\alpha \Rightarrow 0$

Density functional theory

Hohenberg and Kohn, *Phys. Rev*. **136** B864 (1964)
Kohn and Sham, *Phys. Rev*. **140** A1133 (1965)

Mean field approximation: $U_0(\{\mathbf{R}^a\}) \Rightarrow U_0(\{\rho(\mathbf{r})\},\{\mathbf{R}^a\})$

Electron density

Kohn-Sham construction: $\rho(\mathbf{r}) \approx \rho_{KS}(\mathbf{r}) = \sum_n |\psi_n(\mathbf{r})|^2$

$$\mathcal{H}_{\text{KS}}^{\text{Electrons}}(\mathbf{r},\rho(\mathbf{r}),\{\mathbf{R}^a\})\psi_n(\mathbf{r}) = \varepsilon_n\psi_n(\mathbf{r})$$

Independent electron wavefunction

More computational details:

$$\mathcal{H}_{\mathrm{KS}}^{\mathrm{Electrons}}(\mathbf{r},\rho(\mathbf{r}),\{\mathbf{R}^a\}) = -\frac{\hbar^2\nabla^2}{2m} + \underbrace{\sum_a \frac{-Z^a e^2}{|\mathbf{r}-\mathbf{R}^a|}}_{\text{electron-nucleus}} + \underbrace{e^2\int d^3r'\frac{\rho(\mathbf{r}')}{|\mathbf{r}-\mathbf{r}'|}}_{\text{electron-electron}} + \underbrace{V_{xc}\left(\rho(\mathbf{r})\right)}_{\text{exchange-correlation}}$$

Exchange-correlation functionals:

LDA: J. Perdew and Y. Wang, Phys. Rev. B **45**, 13244 (1992)

GGA: J. Perdew, K. Burke, and M. Ernzerhof, PRL **77**, 3865 (1996)

HSE06: J. Heyd, G. E. Scuseria, and M. Ernzerhof, JCP **118**, 8207 (2003)

Numerical methods:

"Muffin-tin" construction: Augmented Plane Wave developed by Slater → "linearized" version by Andersen:

J. C. Slater, Phys. Rev. **51** 846 (1937)

O. K. Andersen, Phys. Rev. B **12** 3060 (1975) (LAPW)

Pseudopotential methods:

J. C. Phillips and L. Kleinman, Phys. Rev. **116** 287 (1959) -- original idea

P. Blöchl, Phys. Rev. B. 50 17953 (1994) – Projector Augmented Wave (PAW) method

Outputs of calculations:

Ground state energy:

$$U_0(\{\rho(\mathbf{r})\},\{\mathbf{R}^a\}) \quad \Rightarrow \quad \text{Determine formation energies}$$

$$\min\Big|_{\{\mathbf{R}^a\}}\left(U_0(\{\rho(\mathbf{r})\},\{\mathbf{R}^a\})\right) \quad \Rightarrow \quad \text{Determine structural parameters}$$

$$\Rightarrow \quad \text{Stable and meta-stable structures}$$

$$\rho_{KS}(\mathbf{r}) = \sum_n |\psi_n(\mathbf{r})|^2 \quad \Rightarrow \quad \text{Self-consistent electron density}$$

$$\{\varepsilon_n\} \quad \Rightarrow \quad \text{One-electron energies; densities of states}$$

Nuclear Hamiltonian (usually treated classically)

$$\mathcal{H}^{\text{Nuclei}}\left(\{\mathbf{R}^a\}\right) = \sum_a \frac{\mathbf{P}^{a2}}{2M^a} + U_0(\{\rho(\mathbf{r})\},\{\mathbf{R}^a\})$$

➔ Normal modes of vibration

Codes used for calculations

Function	Code	Website
Generate atomic datasets	ATOMPAW	http://pwpaw.wfu.edu
DFT; optimize structure	PWscf abinit	http://www.quantum-espresso.org http://www.abinit.org
Structural visualization	XCrySDen VESTA	http://ww.xcrysden.org http://jp-minerals.org/vesta/en/

ATOMPAW Code for generating atomic datasets for PAW calculations

Holzwarth, Tackett, and Matthews, CPC 135 329 (2001) http://pwpaw.wfu.edu

- ATOMPAW
- INFO
- DATASETS
- CONTRIBUTERS
- CONTACT INFO
- NAWH Web
- PHYSICS Web
- WFU Web

ATOMPAW

Download source code and example files:

- atompaw-4.0.0.14.tar.gz (5.4mb) 12/28/2016 NAWH corrected the FINITE-NUCLEUS option for DFT calculations, allowing for models 2, 3, 4, and 5 described by Andrae in Physics Reports **336** 413-525 (2000) .
- atompaw-3.1.0.3.tar.gz (3.8mb) - January 2014 - Older version of atompaw with contributions from Marc Torrent and Francois Jollet as well as several others.
- pwpaw_2.4.tgz (0.2 mb) Updated 05/12/2010 version of *pwpaw* with very minor changes to accomodate changes to input files generated by new *atompaw* output files; also includes a BSD license file.

Atomic PAW datasets:
Comparison with LAPW results for binding energy curves --

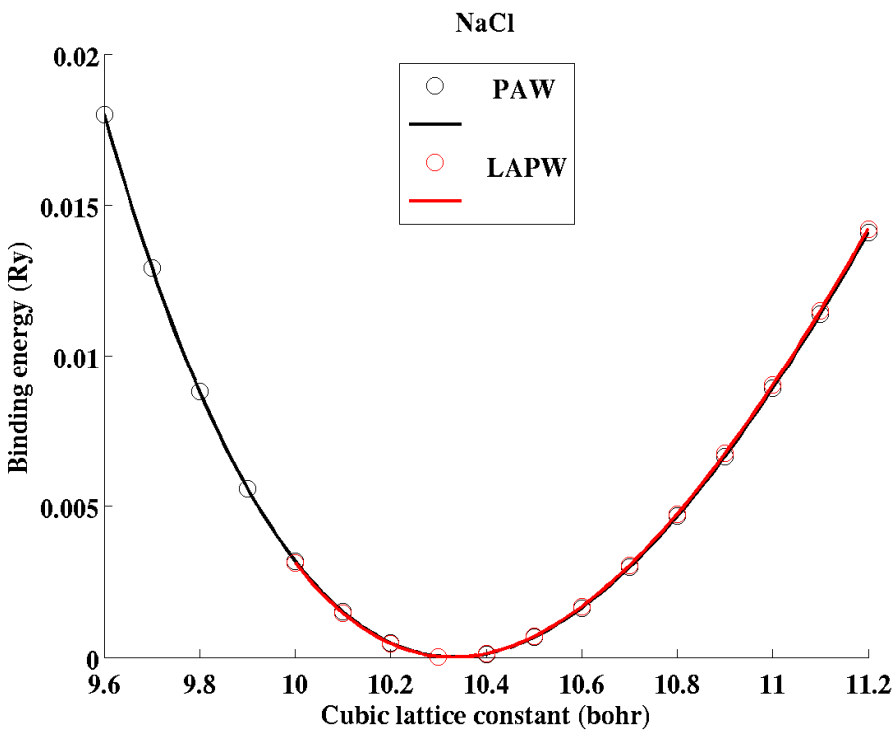

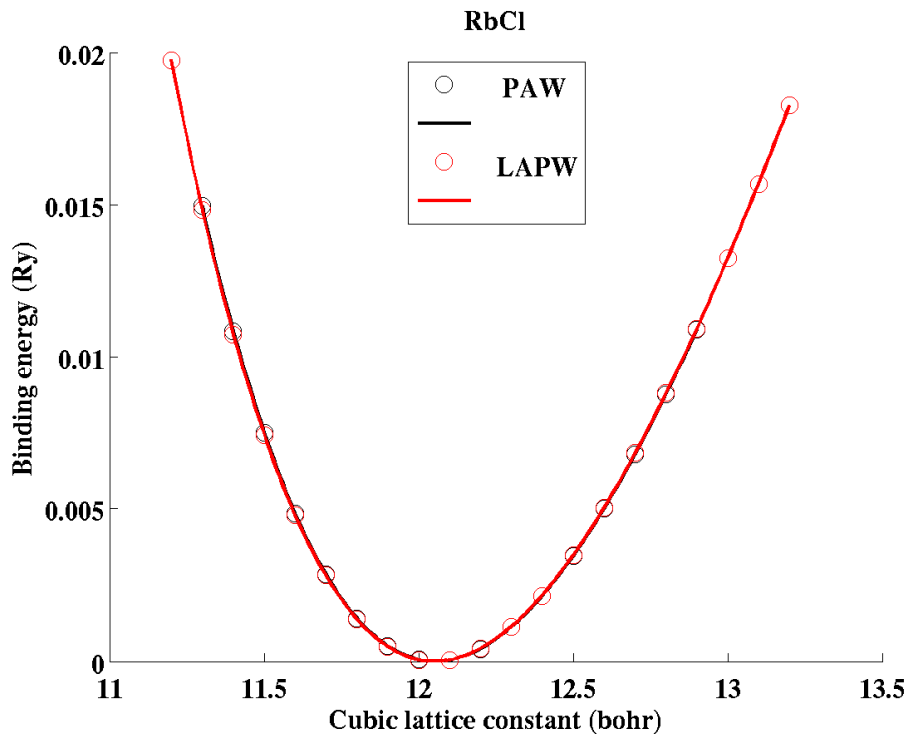

Validation

Li_3PO_4 crystals

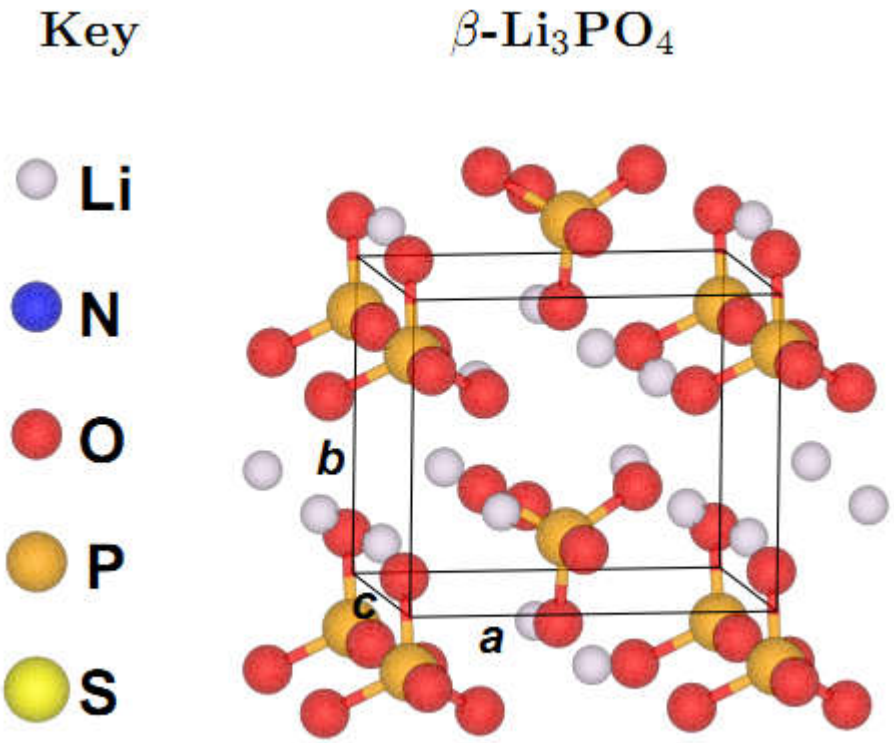

(Pmn2$_1$)

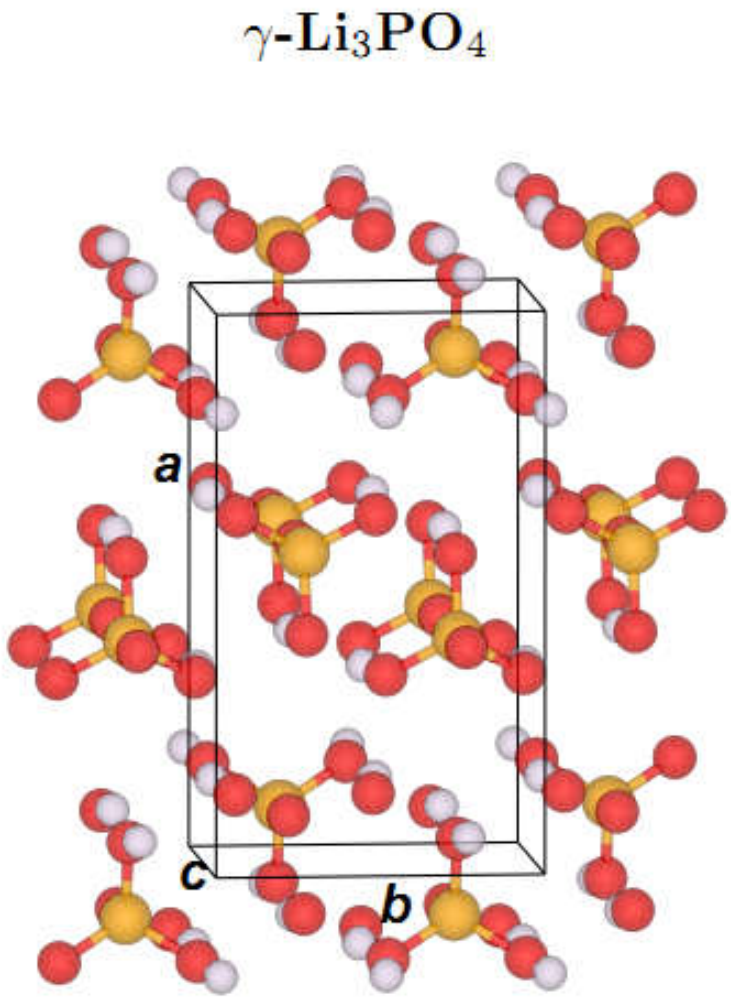

(Pnma)

Validation of calculations

Raman spectra – Experiment & Calculation

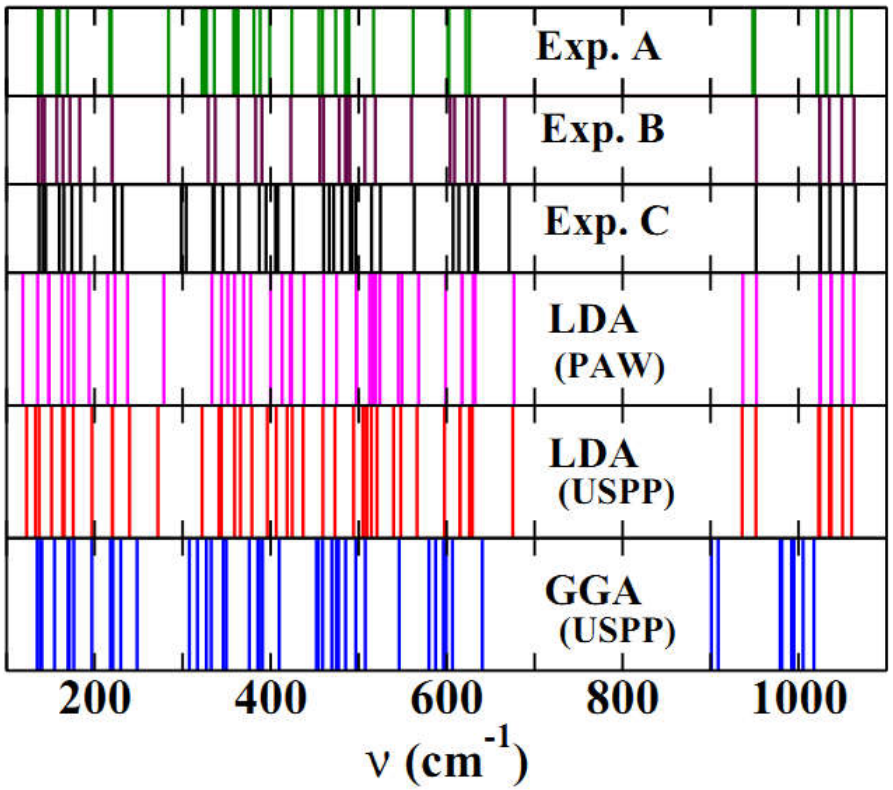

γ-Li_3PO_4

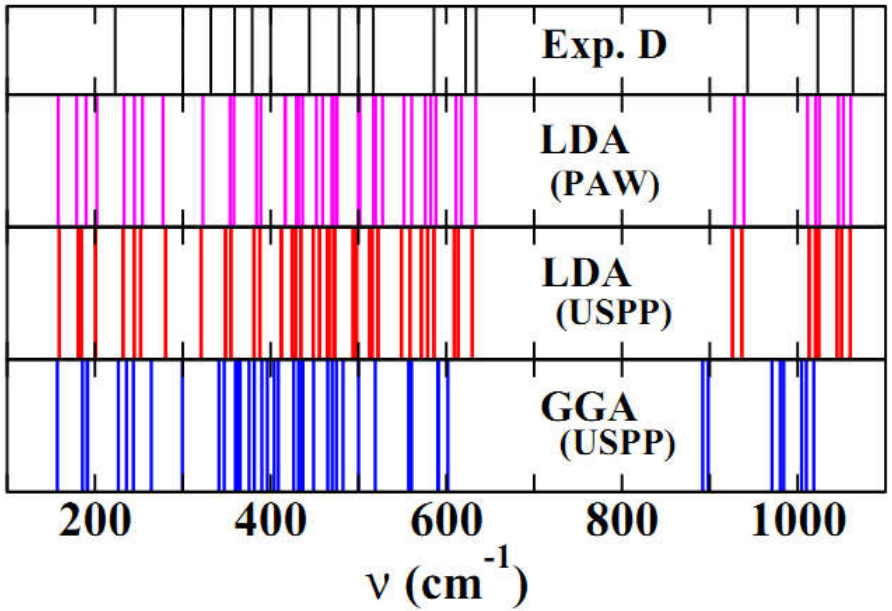

β-Li_3PO_4

A: B. N. Mavrin et al, J. Exp. Theor. Phys. **96**,53 (2003); B: F. Harbach and F. Fischer, Phys. Status Solidi B **66**, 237 (1974) – room temp. C: Ref. B at liquid nitrogen temp.; D: L. Popović et al, J. Raman Spectrosc. **34**,77 (2003).

Heats of formation – Experiment & Calculation

Table 1. Calculated heats of formation for Li phosphates, phospho-nitrides, and thiophosphates and related materials. The structural designation uses the the notation defined in the International Table of Crystallography[85] based on structural information reported in the International Crystal Structure Database.[86] The heats of formation ΔH (eV/FU) are given in units of eV per formula unit. When available from Ref. [31] and [32] experiment values are indicated in parentheses. Those indicated with "*" were used fitting the O and N reference energies as explained in the text.

Material	Structure	ΔH (eV/FU)
β-Li_3PO_4	$Pmn2_1$ (#31)	-21.23
γ-Li_3PO_4	$Pnma$ (#62)	-21.20 (-21.72*)
γ-Li_3PS_4	$Pmn2_1$ (#31)	- 8.37
β-Li_3PS_4	$Pnma$ (#62)	- 8.28
$Li_4P_2O_6$	$P\bar{3}1m$ (#162)	-29.72
$Li_4P_2O_7$	$P\bar{1}$ (#2)	-33.97
$Li_5P_2O_6N$	$P\bar{1}$ (#2)	-33.18
$Li_4P_2S_6$	$P\bar{3}1m$ (#162)	-12.42
$Li_4P_2S_7$	$P\bar{1}$ (#2)	-11.59
$Li_7P_3O_{11}$	$P\bar{1}$ (#2)	-54.84
$Li_7P_3S_{11}$	$P\bar{1}$ (#2)	-20.01
$LiPO_3$	$P2/c$ (#13)	-12.75
$LiPN_2$	$I\bar{4}2d$ (#122)	- 3.65
$s1$-Li_2PO_2N	$Pbcm$ (#57)	-12.35
SD-Li_2PO_2N	$Cmc2_1$ (#36)	-12.47
SD-Li_2PS_2N	$Cmc2_1$ (#36)	- 5.80

Material	Structure	ΔH (eV/FU)
N_2O_5	$P6_3/mmc$ (#194)	- 0.94 (- 0.45*)
P_3N_5	$C2/c$ (#15)	- 3.02 (- 3.32*)
h-P_2O_5	$R3c$ (#161)	-15.45 (-15.53*)
o-P_2O_5	$Fdd2$ (#43)	-15.78
P_2S_5	$P\bar{1}$ (#2)	- 1.93
P_4S_3	$Pnma$ (#62)	- 2.45 (- 2.33)
SO_3	$Pna2_1$ (#33)	- 4.84 (- 4.71*)
Li_3N	$P6/mmm$ (#191)	- 1.60 (- 1.71*)
Li_2O	$Fm\bar{3}m$ (#225)	- 6.10 (- 6.20*)
Li_2O_2	$P6_3/mmc$ (#194)	- 6.35 (- 6.57*)
Li_3P	$P6_3/mmc$ (#194)	- 3.47
Li_2S	$Fm\bar{3}m$ (#225)	- 4.30 (- 4.57)
Li_2S_2	$P6_3/mmc$ (#194)	- 4.09
$LiNO_3$	$R\bar{3}c$ (#167)	- 5.37 (- 5.01*)
Li_2SO_4	$P2_1/c$ (#14)	-14.63 (-14.89*)

Estimate of ionic conductivity assuming activated hopping

Schematic diagram of minimal energy path

Approximated using NEB algorithm[a]
– "Nudged Elastic Band"

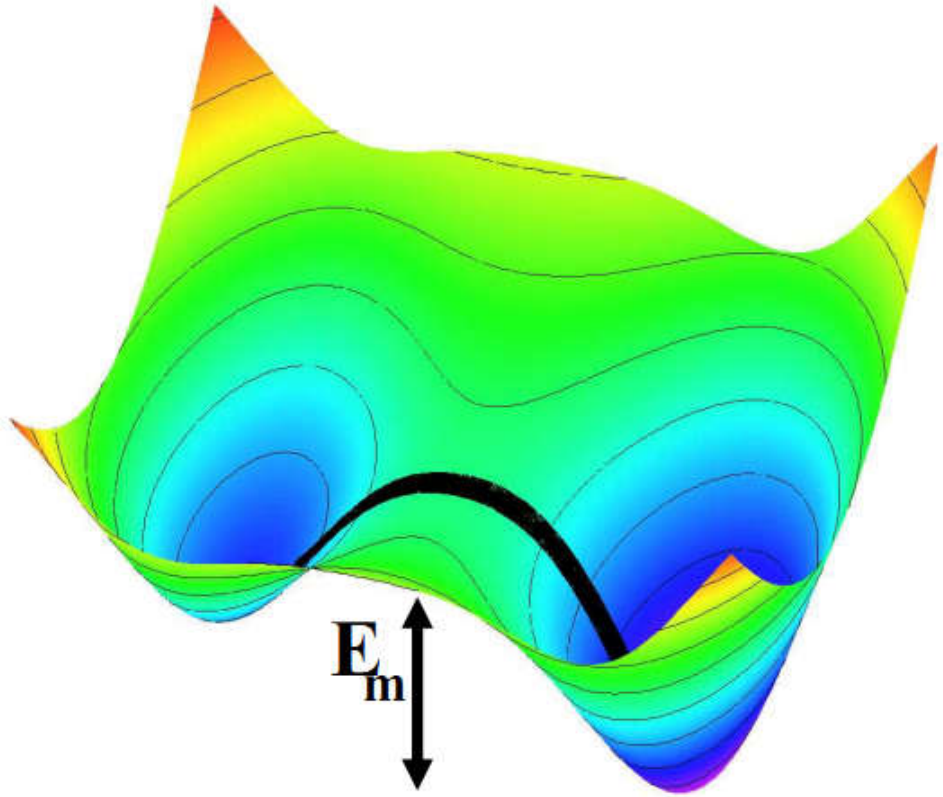

[a] Henkelman and Jónsson, *JCP* **113**, 9978 (2000)

Arrhenius relation

$$\sigma \cdot T = K e^{-E_A/kT}$$

From: Ivanov-Shitz and co-workers, *Cryst. Reports* **46**, 864 (2001):

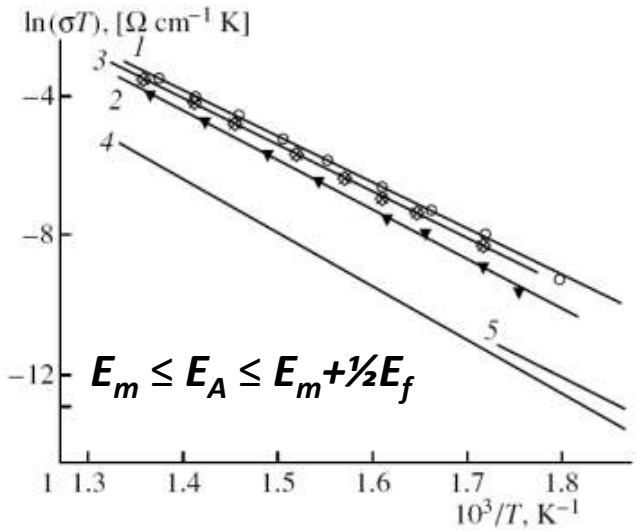

Fig. 2. Temperature dependences of conductivity in γ-Li_3PO_4: (*1–3*) for single crystals measured along the (*1*) *a*-axis, (*2*) *b*-axis, (*3*) *c*-axis and (*4, 5*) for a polycrystal (*4*) according to [4, 5] and (*5*) according to [7].

E_A = 1.14, 1.23, 1.14, 1.31, 1.24 eV for 1,2,3,4,5, respectively.

Arrhenius activation energies – simulation and experiment

	Simulation			Experiment	
Material	E_m *(eV)*	E_f *(eV)*	E_A *(eV)*	E_A *(eV)*	*Ref.*
LiPON				≈0.6	Amorphous
γ-Li_3PO_4	0.3	1.7	1.1	1.13	Single crystal
***SD*-Li_2PO_2N**	0.4	2.0	0.4-1.4	0.6	Poly. crystal
$Li_{14}P_2O_3N_6$	0.3	0.3	0.3-0.4		
Li_7PN_4 +O	0.5	-	0.5	0.48	Poly. crystal
β-Li_3PS_4	0.2	0.0	0.2	0.4	Poly. crystal
$Li_7P_2S_{11}$	0.2	0.0	0.2	0.1	Poly. crystal

➢What is meant by "first principles"?

A series of well-controlled approximations

- ❑ Born-Oppenheimer Approximation
- ❑ Density Functional Approximation
- ❑ Local density Approximation (LDA)
- ❑ Numerical method: Projector Augmented Wave

Validation

- ❑ Lattice vibration modes
- ❑ Heats of formation
- ❑ Activation energies for lattice migration

How can computer simulations contribute to the development of materials?

- Computationally examine known materials and predict new materials and their properties
  - Structural forms
  - Relative stabilities
  - Direct comparisons of simulations and experiment
  - Investigate properties that are difficult to realize experimentally

Of particular interest in battery materials --

- Model ion migration mechanisms
  - Vacancy migration
  - Interstitial migration
  - Vacancy-interstitial formation energies
- Model ideal electrolyte interfaces with anodes

Systematic study of LiPON materials – $Li_xPO_yN_z$ – (Yaojun A. Du and N. A. W. Holzwarth, Phys. Rev. B 81, 184106 (2010))

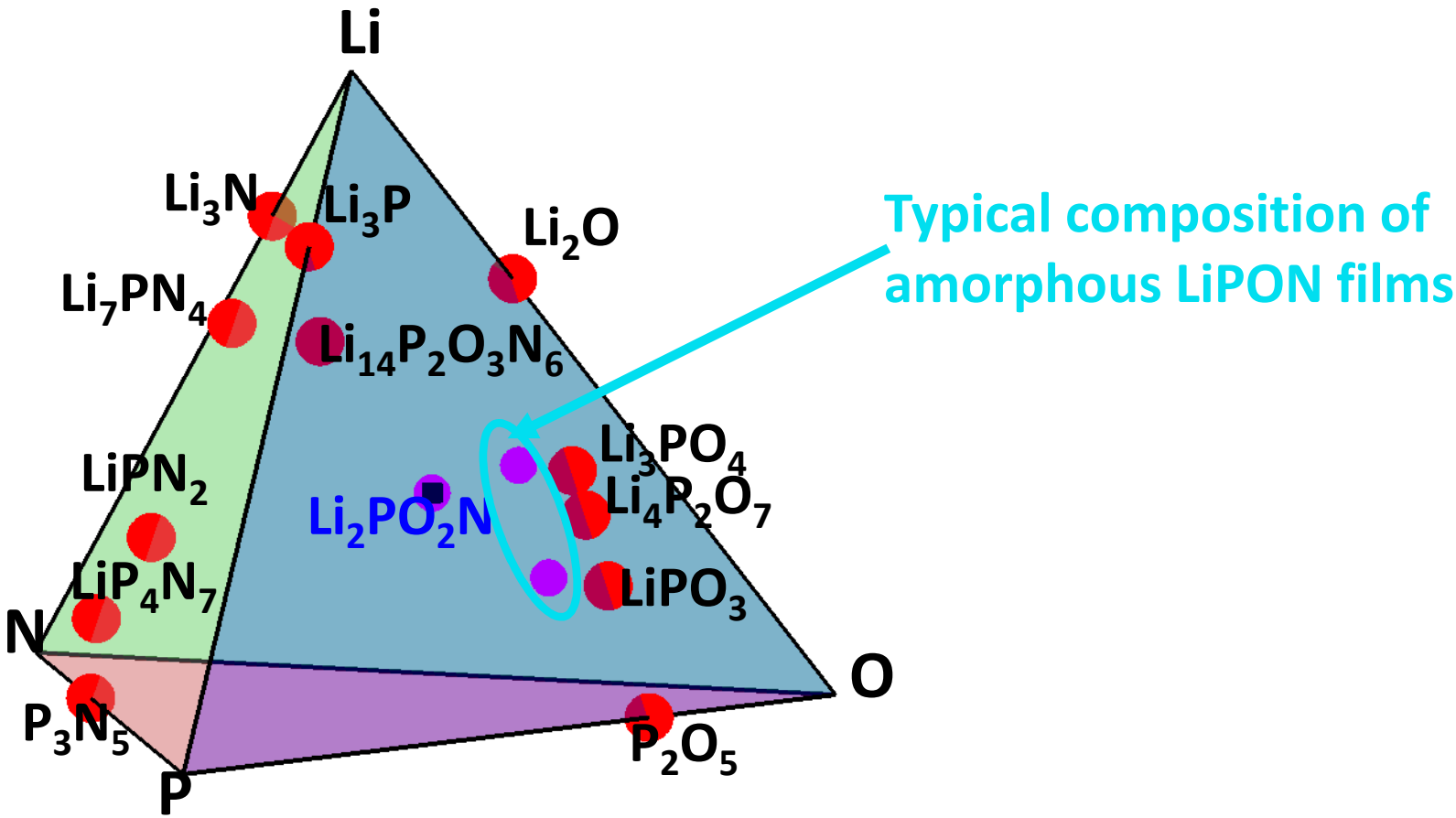

Experimentally known structure

$LiPO_3$

Computationally predicted structure

s_1-Li_2PO_2N

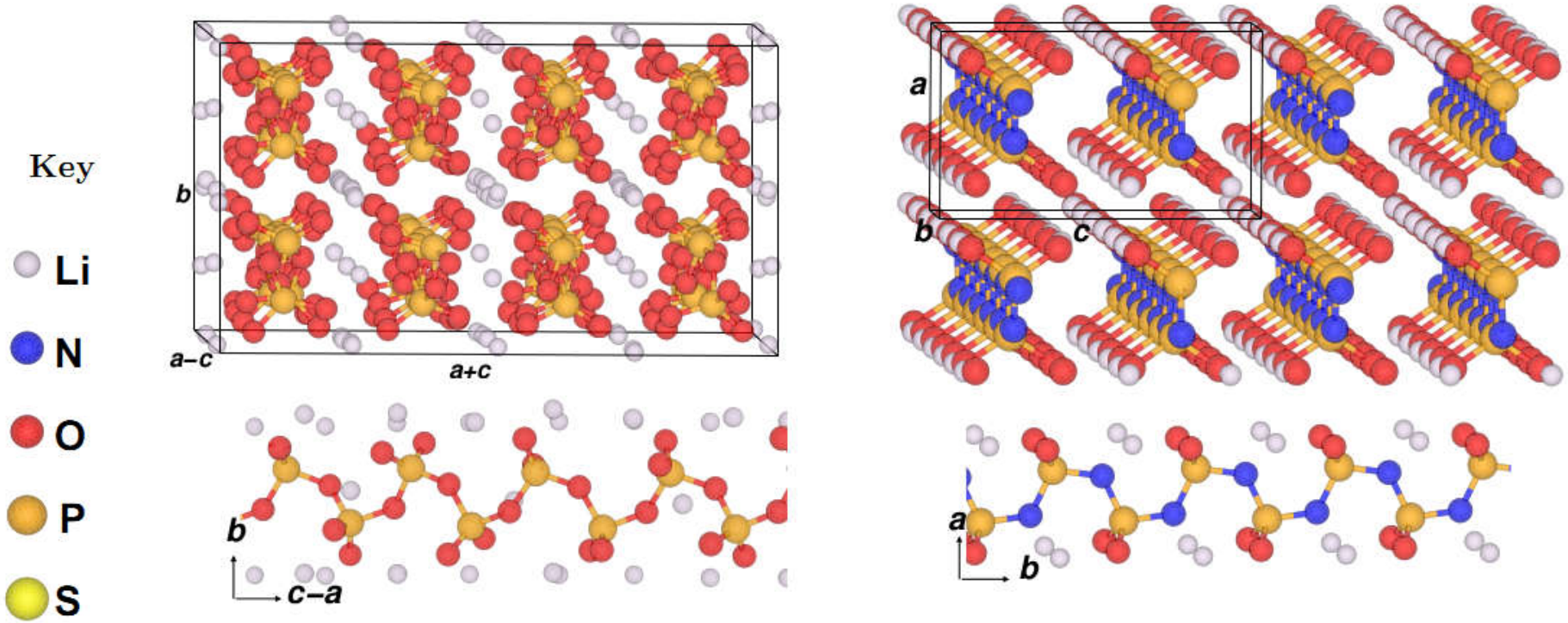

Fig. 7. Ball and stick diagrams for $LiPO_3$ in the $P2/c$ structure (20 formula units per unit cell) and $s1$-Li_2PO_2N in the $Pbcm$ structure (4 formula units per unit cell) from the calculated results. For each crystal diagram, a view of a horizontal chain axis is also provided for a single phosphate or phospho-nitride chain.

Computationally predicted structure

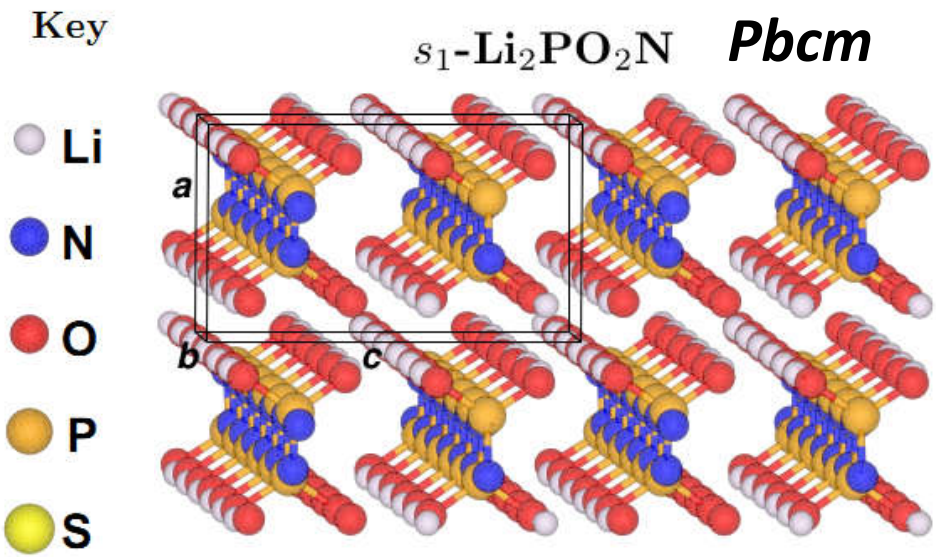

Calculations have now verified that the *SD* structure is more stable than the s_1 structure by 0.1 eV/FU.

Experimentally realized structure

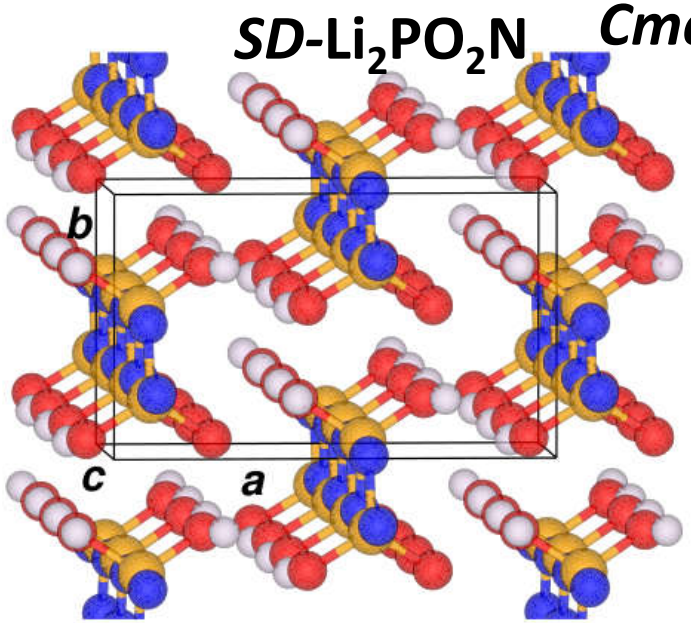

Synthesis of Li_2PO_2N by Keerthi Senevirathne, Cynthia Day, Michael Gross, and Abdessadek Lachgar (*SSI* 233, 95-101 (2013))

High temperature solid state synthesis using reaction:

$$Li_2O + \tfrac{1}{5}P_2O_5 + \tfrac{1}{5}P_3N_5 \rightarrow Li_2PO_2N$$

Comparison of synthesized Li_2PO_2N with Li_2SiO_3

***SD*-Li_2PO_2N (*Cmc2$_1$*)**

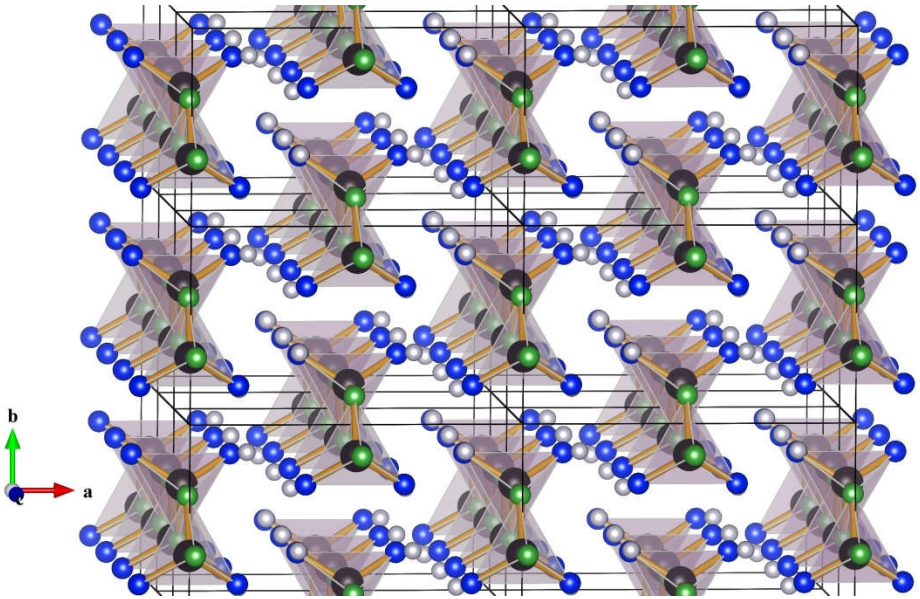

a=9.07 Å, b=5.40 Å, c=4.60 Å

Li_2SiO_3 (*Cmc2$_1$*)

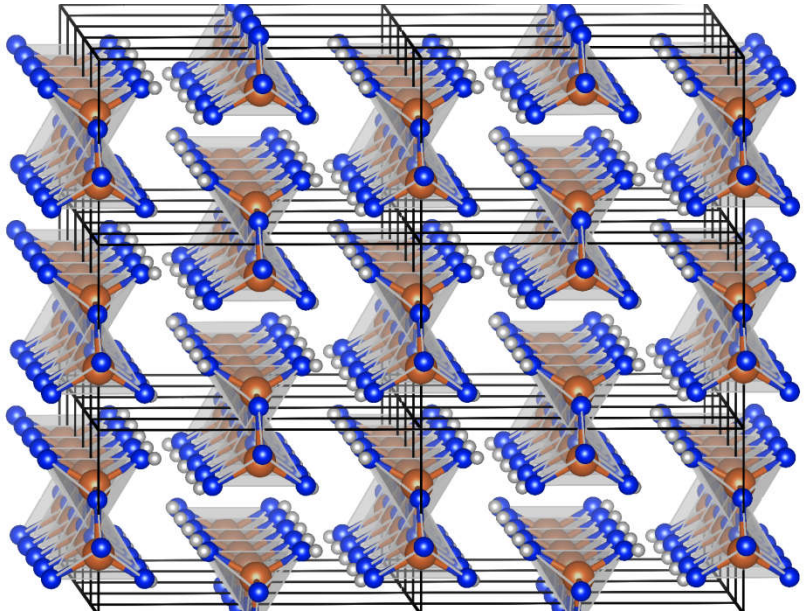

a=9.39 Å, b=5.40 Å, c=4.66 Å

K.-F. Hesse, Acta Cryst. B33, 901 (1977)

Li P O N Si

Ionic conductivity of *SD*-Li_2PO_2N

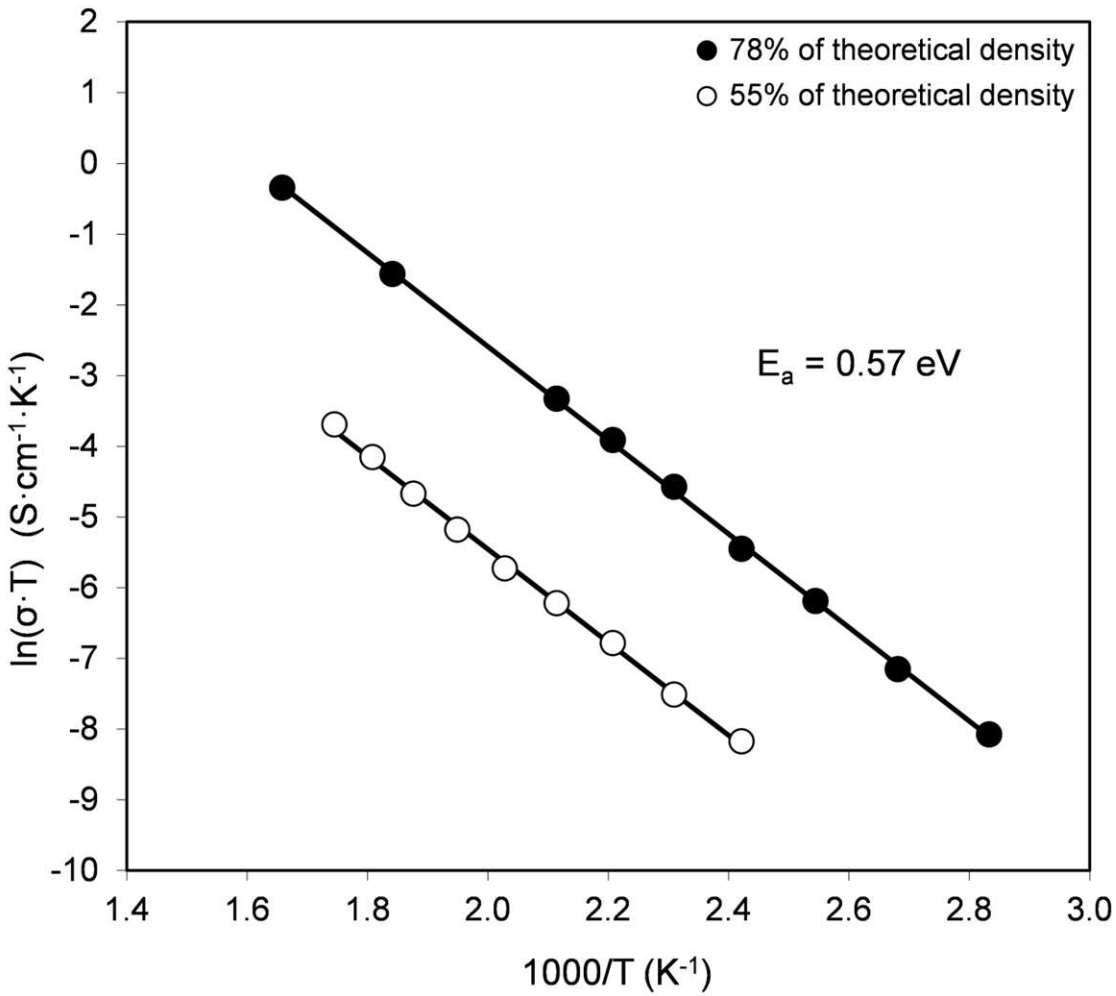

$$\sigma \approx 10^{-6}\ \text{S/cm} \quad \text{at } 80^{o}\ \text{C}$$

NEB analysis of E_m (vacancy mechanism)

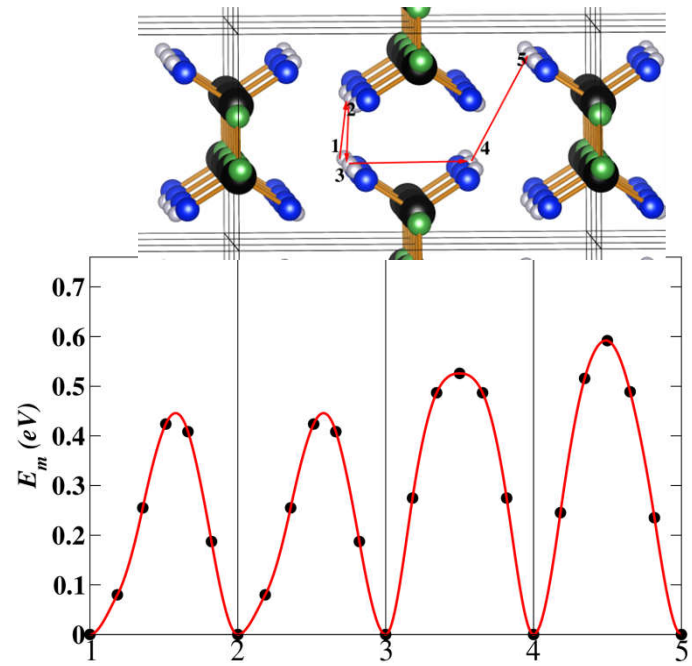

$$E_m \approx 0.4\ \text{eV}; E_f \approx 2\ \text{eV}$$

$$\Rightarrow E_A = E_m + \tfrac{1}{2}E_f \approx 1.4\ \text{eV}$$

➔Sample has appreciable population of vacancies

Summary of the Li_2PO_2N story

- Predicted on the basis of first principles theory
- Subsequently, experimentally realized by Keerthi Senevirathne and colleagues; generally good agreement between experiment and theory
- Ion conductivity properties not (yet) competitive
- Crystalline *SD*-Li_2PO_2N *(Cmc2$_1$)* is quite different from the amorphous LiPON electrolyte developed at ORNL

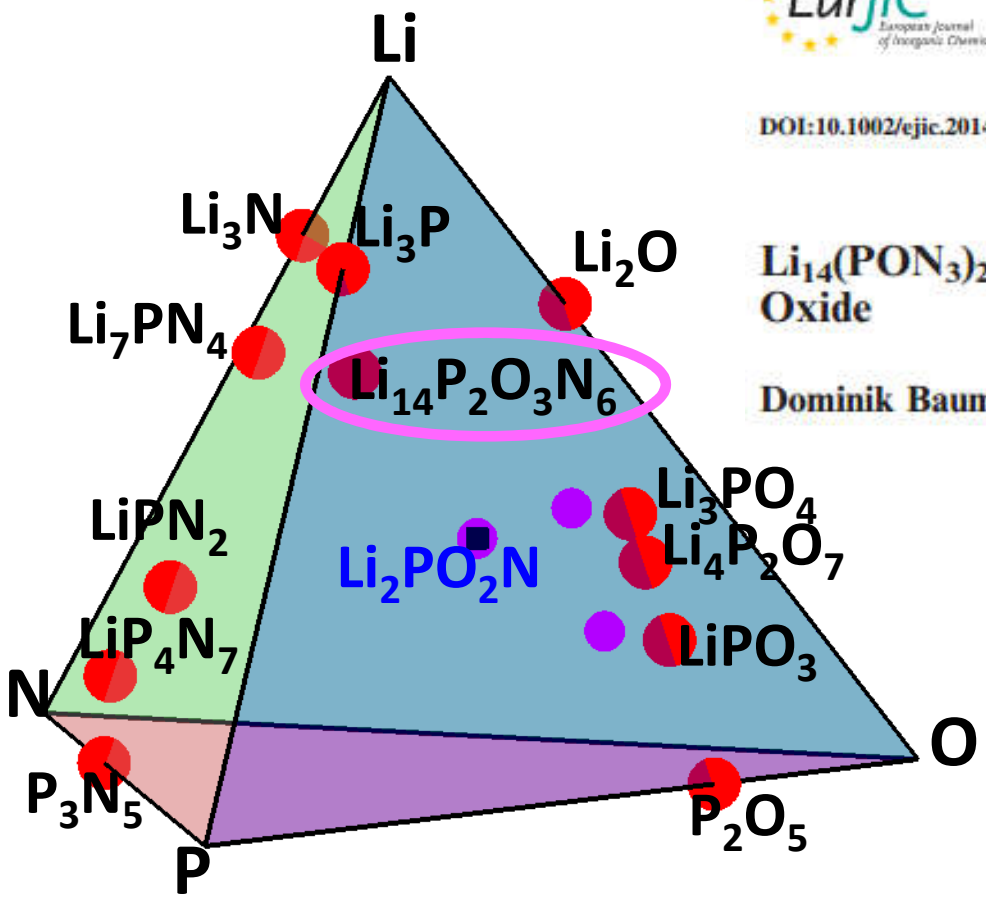

EurJIC European Journal of Inorganic Chemistry
ChemPubSoc Europe

DOI:10.1002/ejic.201403125

$Li_{14}(PON_3)_2O$ – A Non-Condensed Oxonitridophosphate Oxide

Dominik Baumann[a] and Wolfgang Schnick*[a]

***European Journal of Inorganic Chemistry* 2015**, 617-621 (2015)

$Li_{14}P_2O_3N_6$ *($P\bar{3}$)*

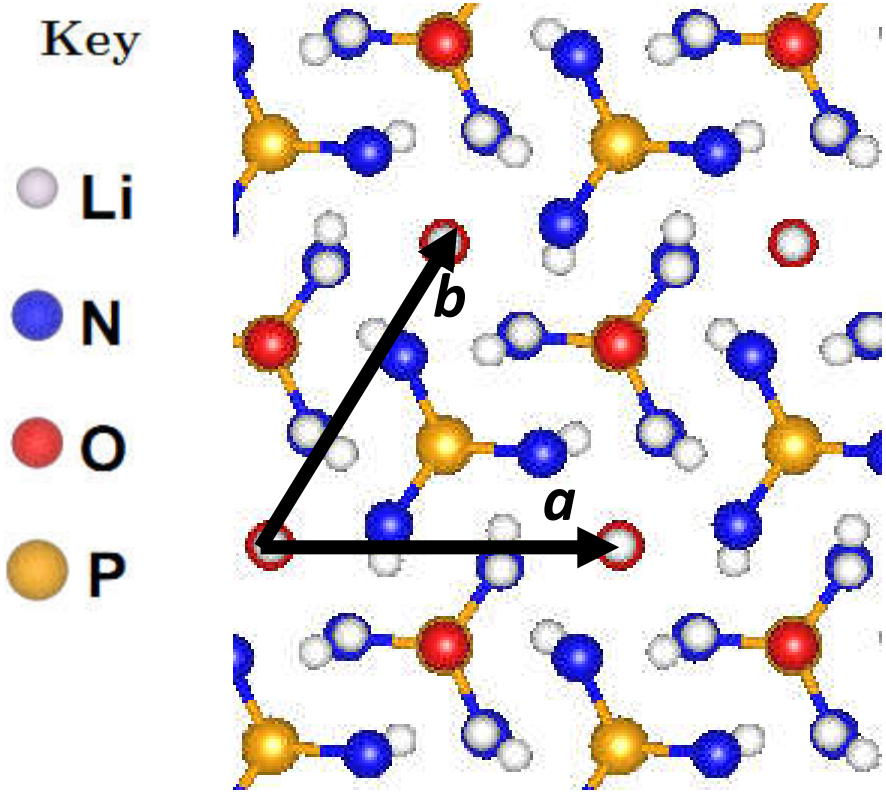

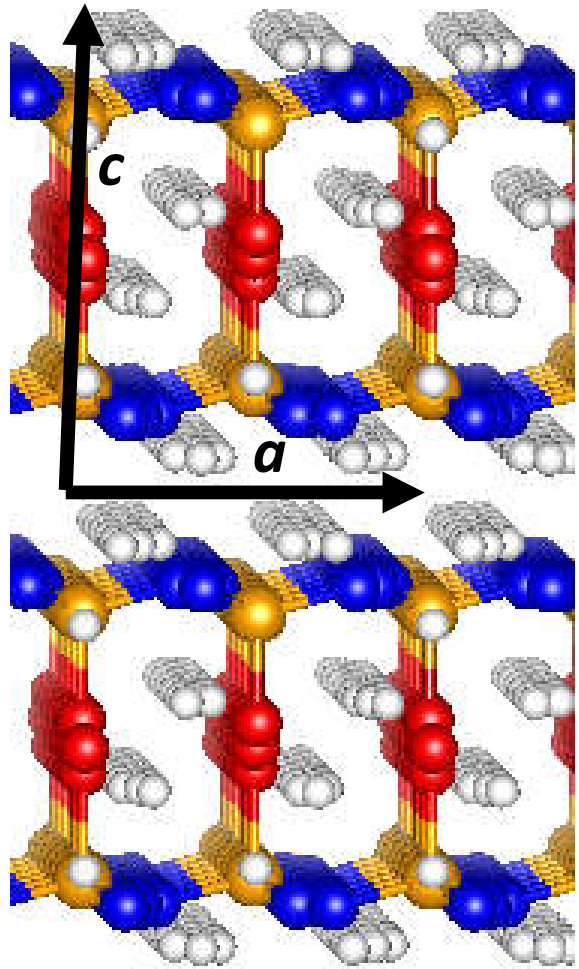

Comparison of partial densities of states of various $Li_xPO_yN_z$ materials

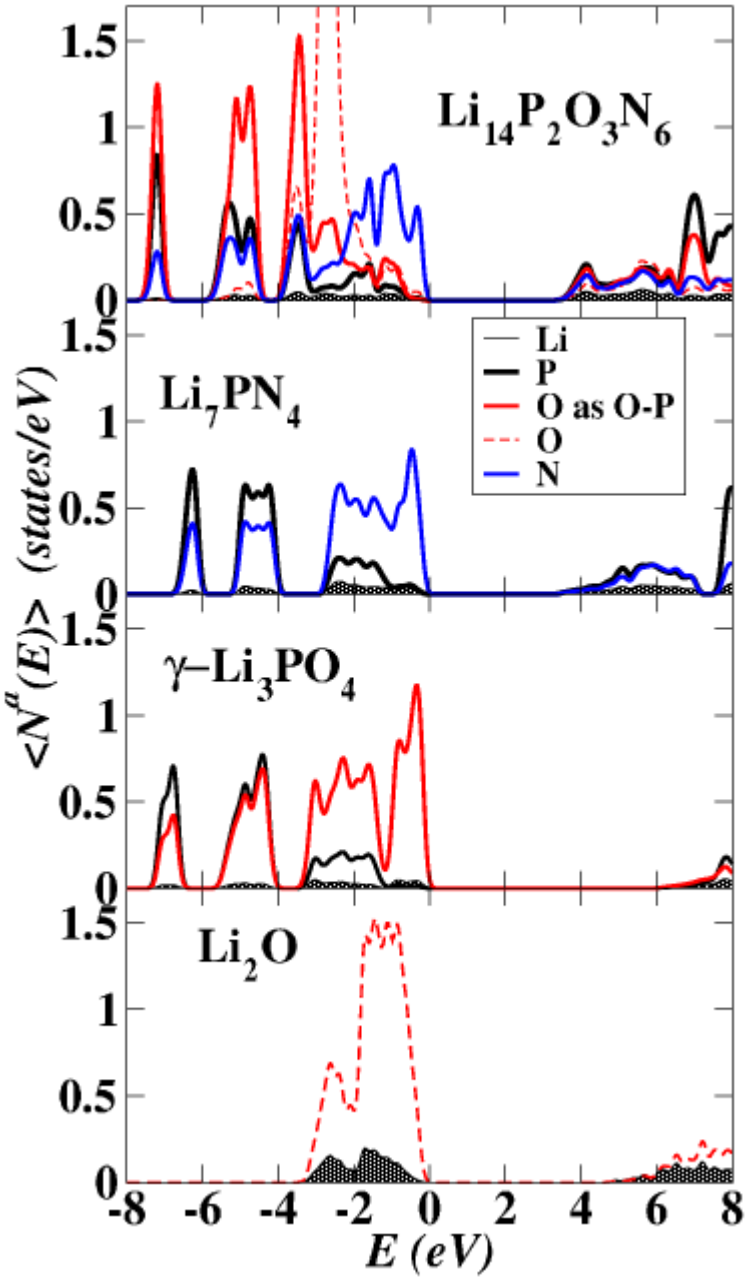

Arrhenius activation energies – simulation and experiment

	Simulation			Experiment	
Material	E_m *(eV)*	E_f *(eV)*	E_A *(eV)*	E_A *(eV)*	*Ref.*
LiPON				≈0.6	Amorphous
γ-Li_3PO_4	0.3	1.7	1.1	1.13	Single crystal
***SD*-Li_2PO_2N**	0.4	2.0	0.4-1.4	0.6	Poly. crystal
$Li_{14}P_2O_3N_6$	0.3	0.3	0.3-0.4		
Li_7PN_4 +O	0.5	-	0.5	0.48	Poly. crystal
β-Li_3PS_4	0.2	0.0	0.2	0.4	Poly. crystal
$Li_7P_2S_{11}$	0.2	0.0	0.2	0.1	Poly. crystal

Other electrolyte materials -- thiophosphate

LiPON and LiS_2-P_2S_5 conductivities

X. Yu, J. B. Bates, G. E. Jellison, Jr., and F. X. Hart, J. Electrochem. Soc. **144** 524-532 (1997):

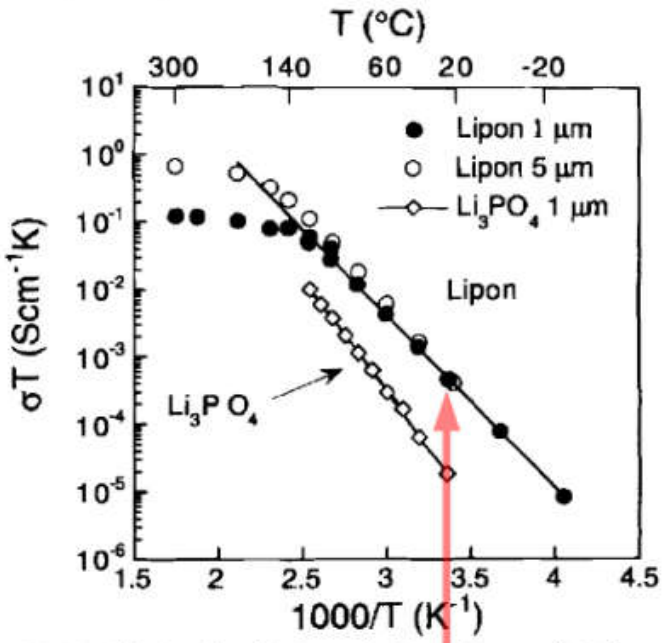

Fig. 3. Arrhenius plot of ionic conductivity of Lipon and Li_3PO_4 vs. temperature.

$\sigma = 2 \times 10^{-6}$ S/cm
$E_a = 0.5$ eV

M. Tatsumisago and A. Hayashi, J. Non-Cryst. Solids **354** 1411-1417 (2008):

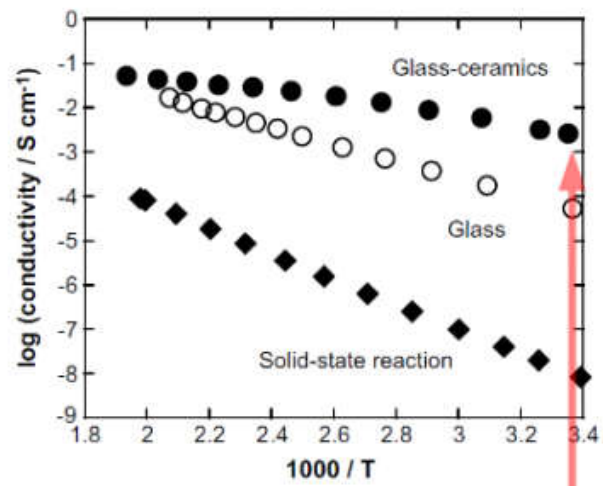

Fig. 5. Temperature dependences of the conductivities for the $70Li_2S \cdot 30P_2S_5$ glass and glass–ceramics. The conductivity data for the sample prepared by solid-state reaction are also shown.

$\sigma = 3 \times 10^{-3}$ S/cm
$E_a = 0.1$ eV

Systematic study of Li_xPS_y materials – (N. D. Lepley and N. A. W. Holzwarth, J. Electrochem. Soc. 159, A538 (2012), Phys. Rev. B 88, 104103 (2013))

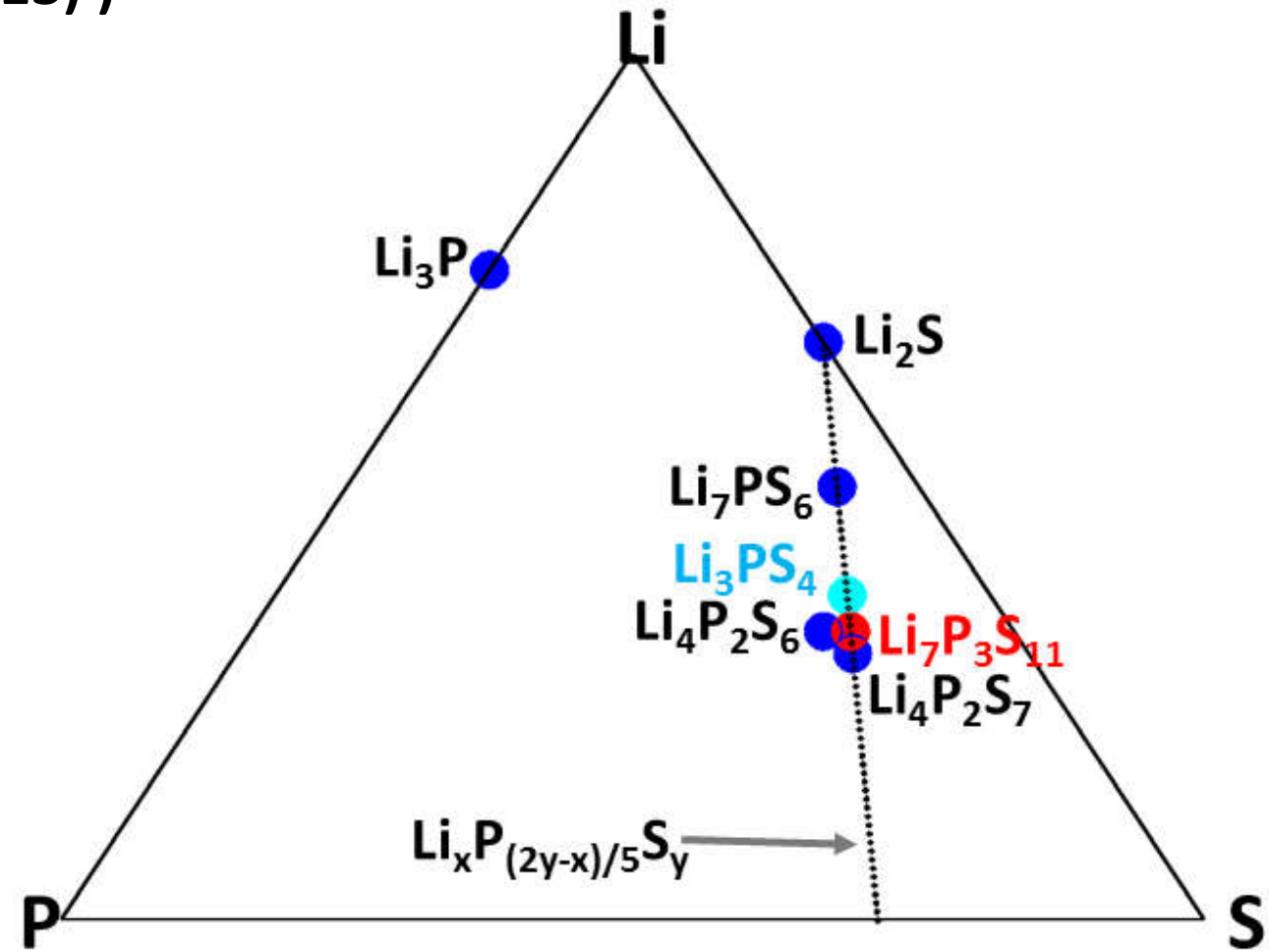

Comparison of some lithium phosphates and thiophosphates

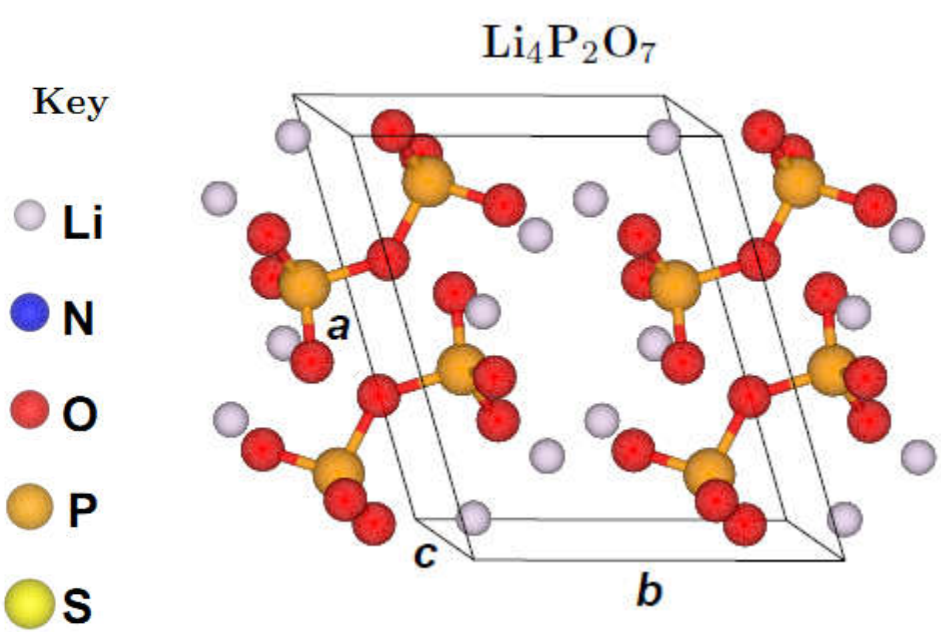

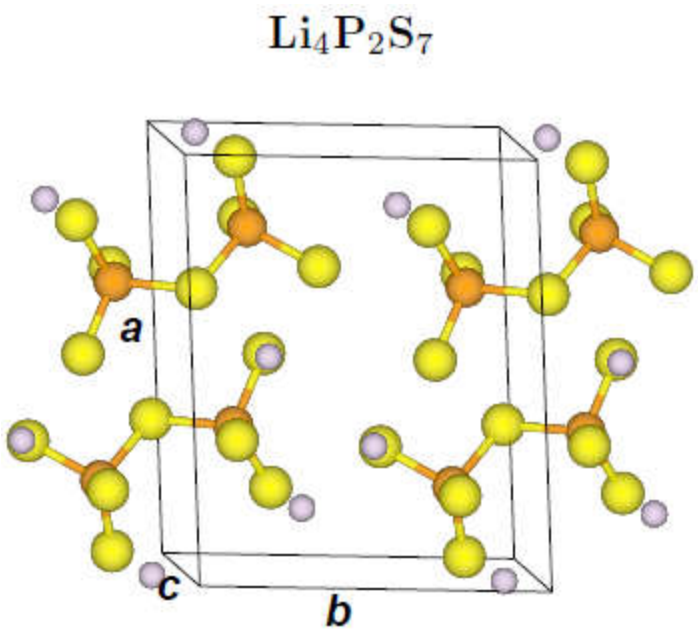

Crystallizes (experimentally and computationally) into $P\bar{1}$ structure

Experimentally amorphous; computationally metastable in $P\bar{1}$ structure

Some lithium thiophosphate crystal structures

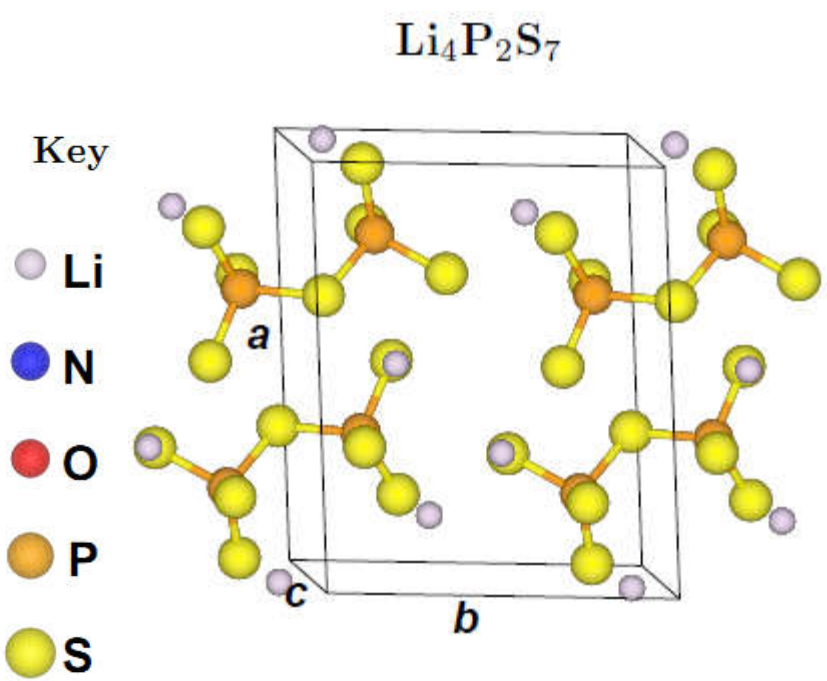

Experimentally amorphous; computationally metastable in $P\bar{1}$ structure

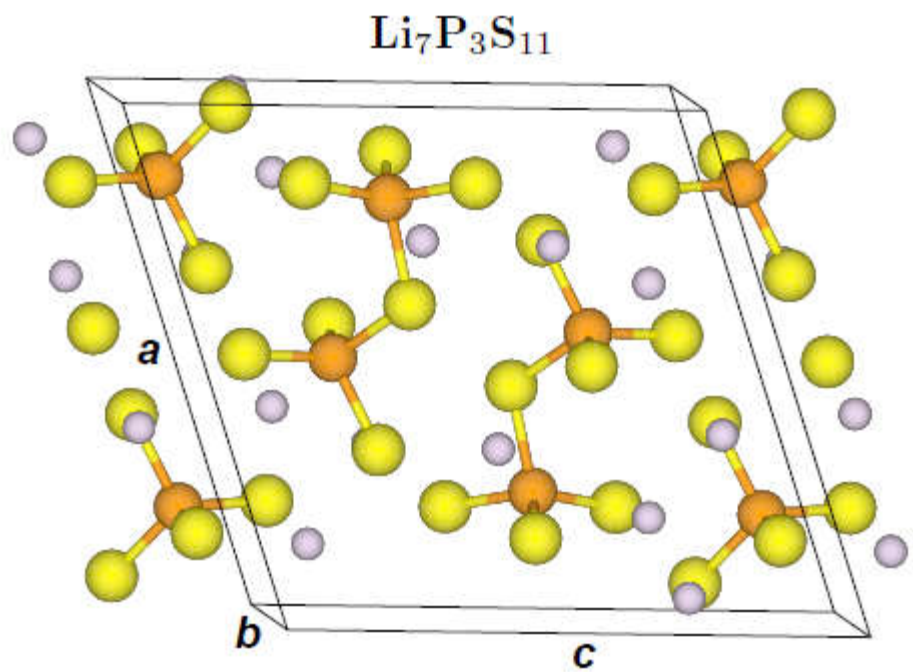

Experimentally and computationally metastable in $P\bar{1}$ structure

Vacancy migration analysis from NEB results for $Li_7P_3S_{11}$: Lepley & Holzwarth, *JECS* **159**, A538-A547 (2012)

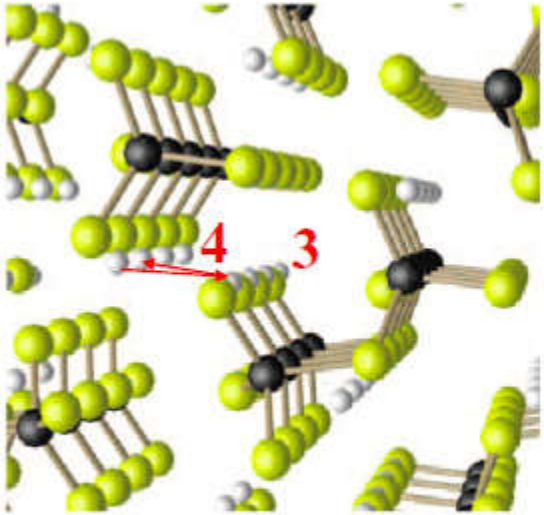

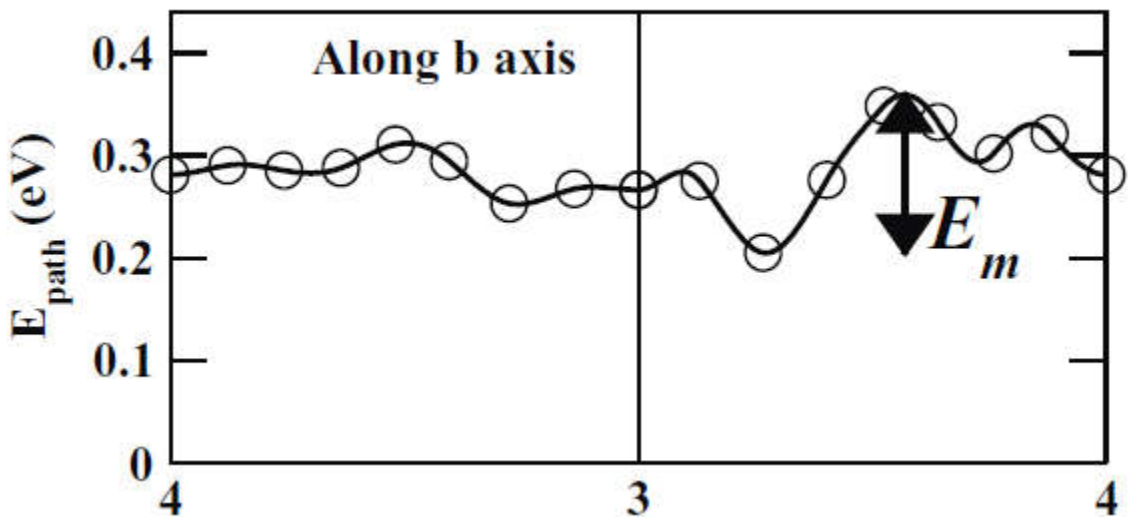

● Li ● P ● S

$$E_m \approx 0.15 \text{ eV}; E_f \approx 0 \text{ eV}$$

$$\Rightarrow E_A = E_m + \tfrac{1}{2} E_f \approx 0.15 \text{ eV}$$

Experiment -- A Hayashi *et al.,* J. Solid State Electrochem. **14**, 1761 (2010):

$$\sigma \approx 2 - 3 \times 10^{-3} \text{ S/cm} \qquad E_A \approx 0.12 - 0.18 \text{ eV}$$

From ORNL: Experiment on electrolyte Li_3PS_4

WAKE FOREST UNIVERSITY

JACS
JOURNAL OF THE AMERICAN CHEMICAL SOCIETY

Communication

pubs.acs.org/JACS

Anomalous High Ionic Conductivity of Nanoporous β-Li_3PS_4

Zengcai Liu,[†] Wujun Fu,[†] E. Andrew Payzant,[†,‡] Xiang Yu,[†] Zili Wu,[†,§] Nancy J. Dudney,[‡] Jim Kiggans,[‡] Kunlun Hong,[†] Adam J. Rondinone,[†] and Chengdu Liang*,[†]

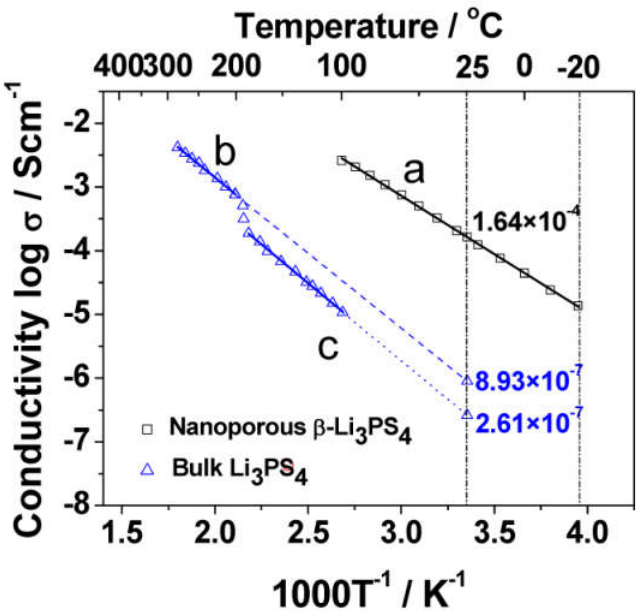

Figure 1. Arrhenius plots for nanoporous β-Li_3PS_4 (line a), bulk β-Li_3PS_4 (line b), and bulk γ-Li_3PS_4 (line c). The conductivity data for bulk Li_3PS_4 are reproduced from the work of Tachez.[10].

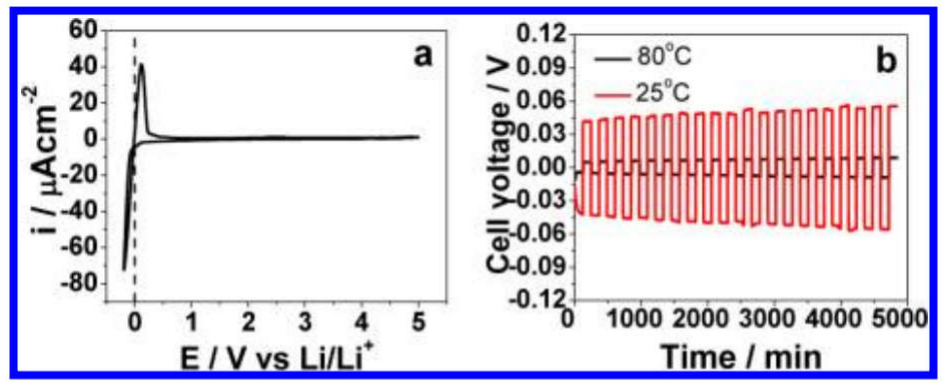

Figure 5. Electrochemical stability of β-Li_3PS_4 and cycling stability with metallic lithium electrodes. (a) CV of a Li/β-Li_3PS_4/Pt cell, where Li and Pt serve as the reference/counter and working electrodes, respectively. (b) Lithium cyclability in a symmetric Li/β-Li_3PS_4/Li cell. The cell was cycled at a current density of 0.1 mA cm^{-2} at room temperature and 80 °C.

β-Li_3PS_4

Li P S

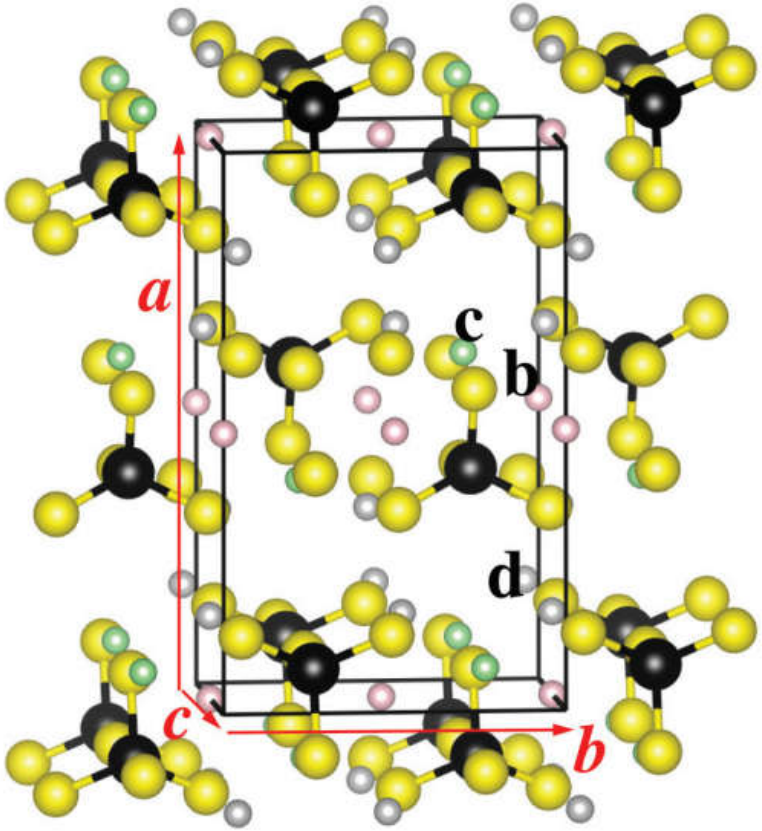

$$E_m \approx 0.2 \text{ eV}; \; E_f \approx 0.0 \text{ eV}$$

$$E_A = E_m + \tfrac{1}{2} E_f \approx 0.2 \text{ eV}$$

$$E_{exp} = 0.4 - 0.5 \text{ eV}$$

γ-Li_3PS_4

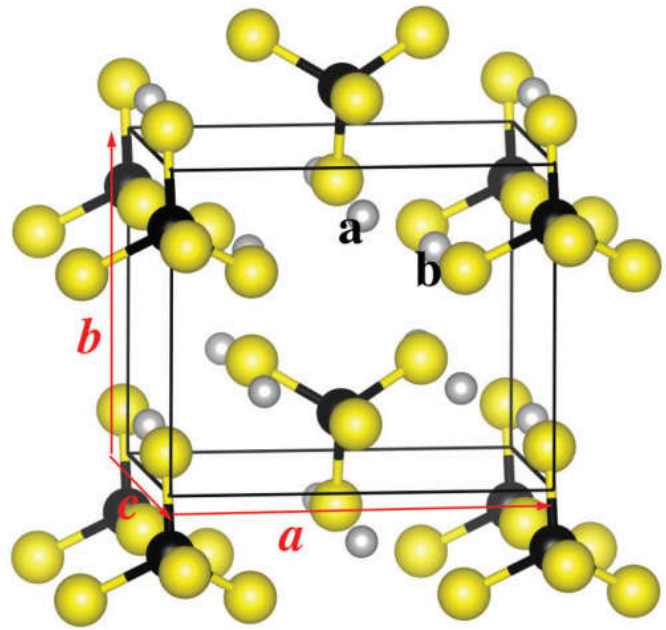

$$E_m \approx 0.3 \text{ eV}; \; E_f \approx 0.8 \text{ eV}$$

$$E_A = E_m + \tfrac{1}{2} E_f \approx 0.7 \text{ eV}$$

$$E_{exp} = 0.5 \text{ eV}$$

Lepley, Du, and Holzwarth, *PRB* **88**, 104103 (2013)

Summary of the Li_xPS_y story

- Simulations verify that thiophosphates have better ion mobility properties than their phosphate analogs
- Meta-stable crystalline $Li_7P_3S_{11}$ has been shown to have particularly favorable ion migration pathways
- γ- and β-Li_3PS_4 have very similar structures, but simulations show their ion mobilities to be different.

Models of Idealized Interfaces

Crystal structure of bulk Li_3PS_4 – γ-form $Pmn2_1$ (#31)

Note: Li_3PS_4 is also found in the β-form with Pnma (#62) structure

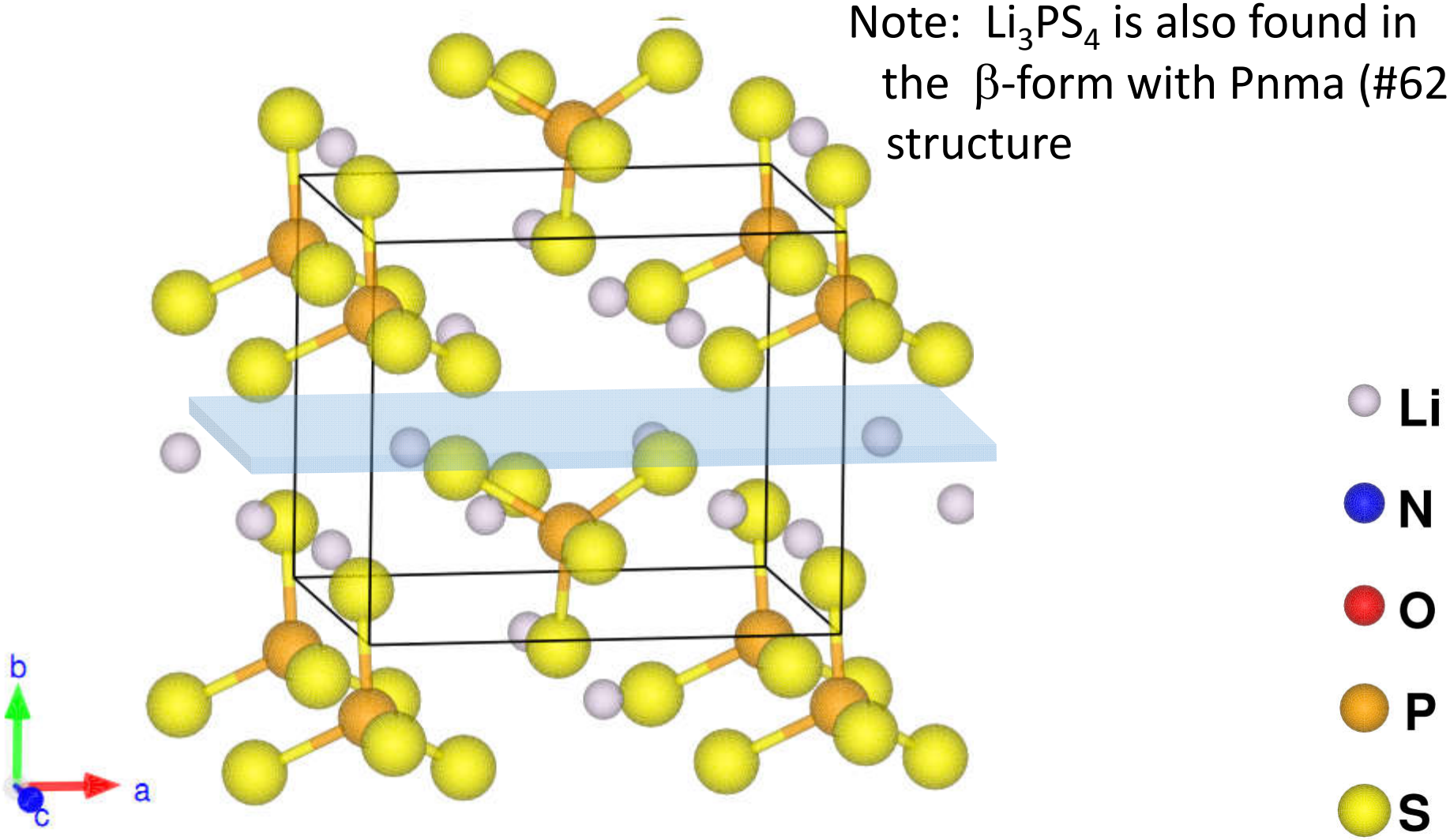

γ-Li_3PS_4 [0 1 0] surface

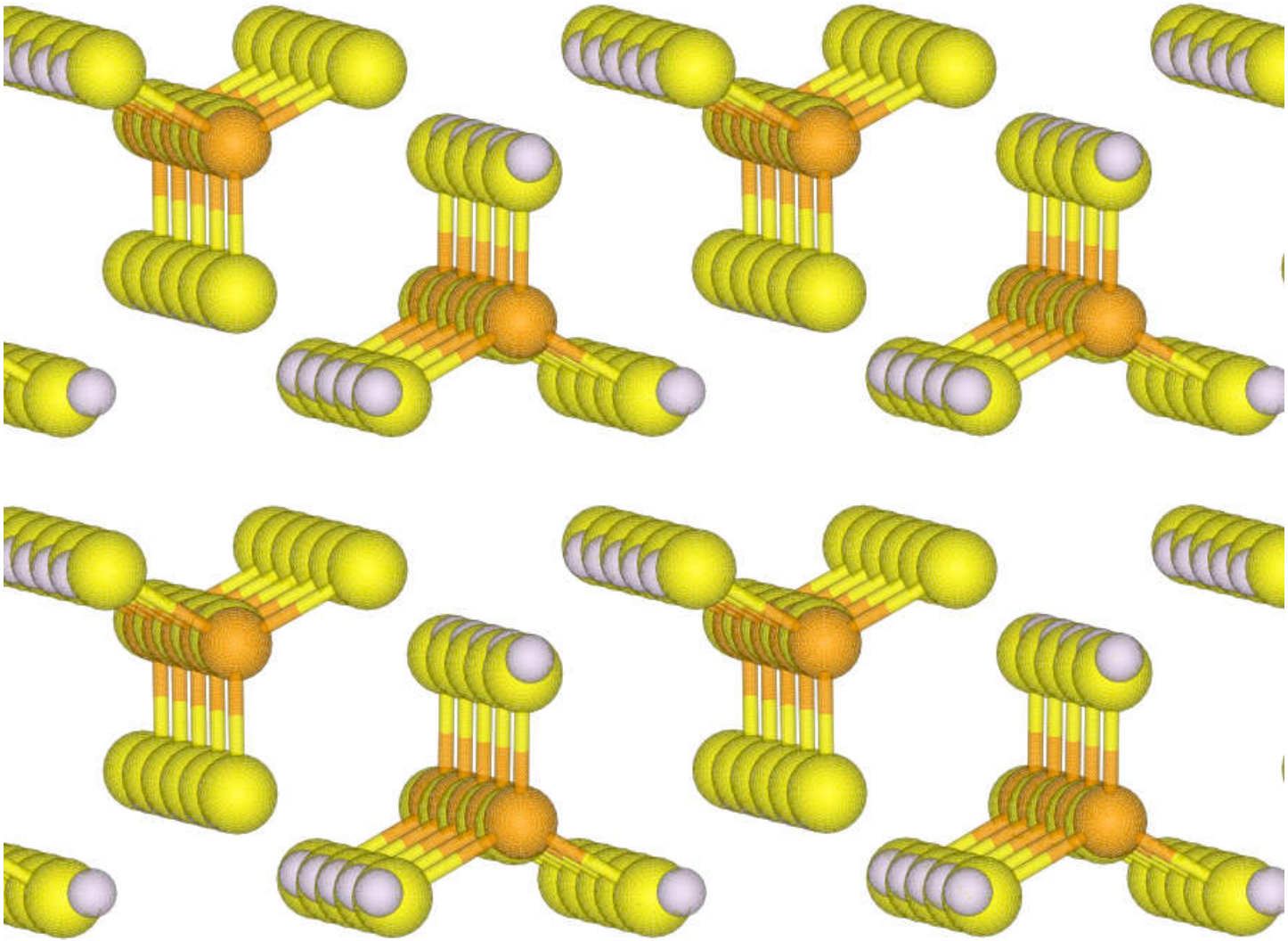

Simulations of ideal γ-Li_3PS_4 [0 1 0] surface in the presence of Li

Initial configuration:

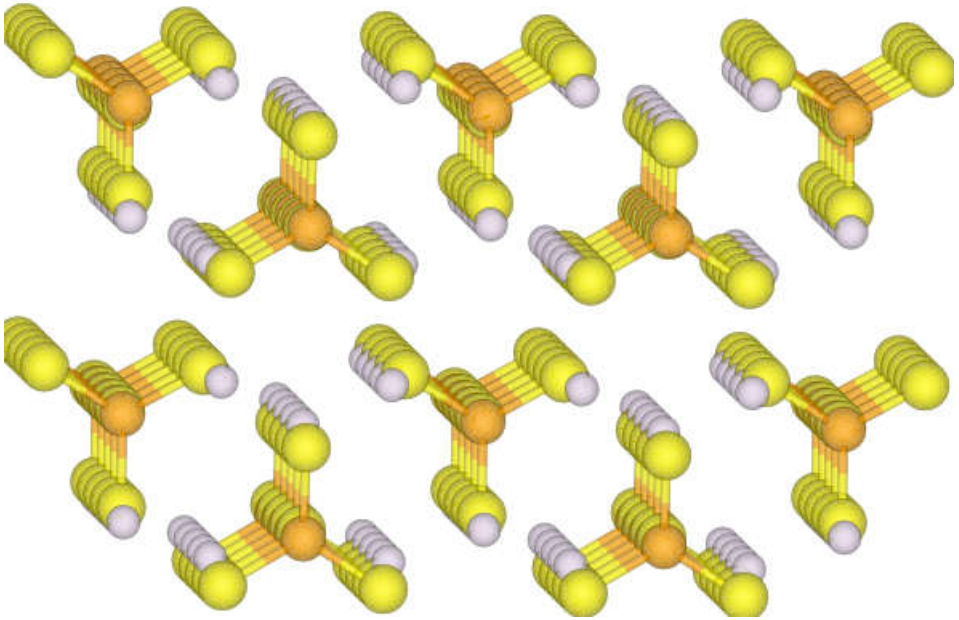

Computed optimized structure:

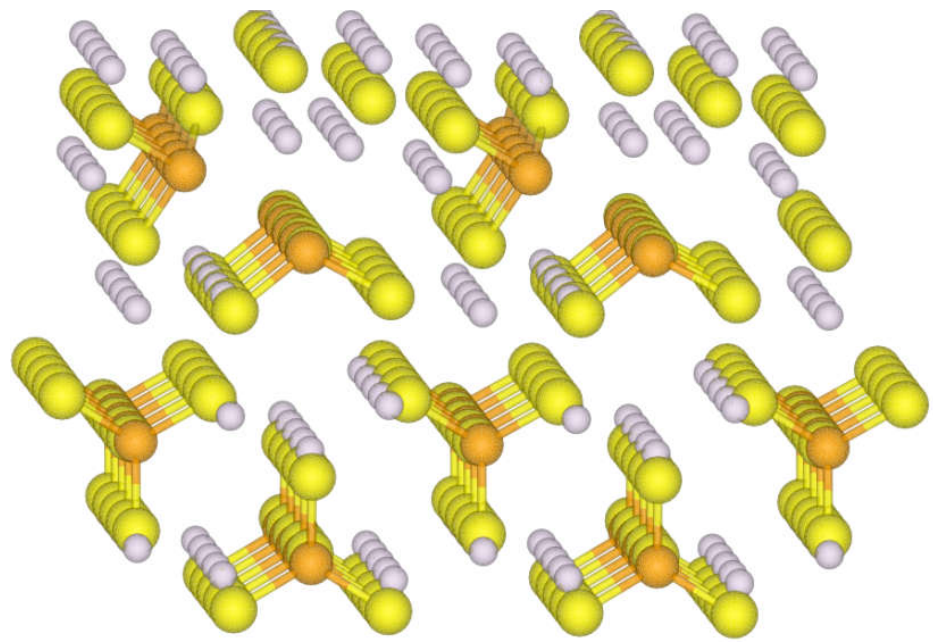

Quantitative study of interfaces – (Lepley & Holzwarth, *PRB* **92** 214201 (2015))

Within any given periodic simulation cell with n_a units of material a and with n_b units of material b, we can define an interface energy:

$$\tilde{\gamma}_{ab}\left(\tilde{\Omega}, n_a, n_b\right) = \frac{\tilde{E}_{ab}\left(\tilde{\Omega}, A, n_a, n_b\right) - n_a E_a - n_b E_b}{A}$$

area of interface within supercell

bulk energies

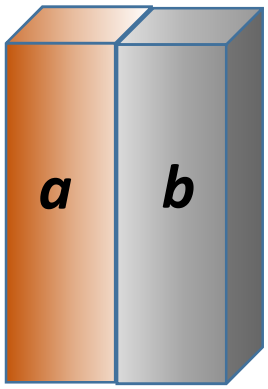

In order approximately remove the effects of lattice strain:

- Design the supercell to be commenserate with lattice a
- Now the strain will scale with the amount of material b

$$\Rightarrow \tilde{\gamma}_{ab}\left(\tilde{\Omega}, n_a, n_b\right) = \tilde{\gamma}_{ab}^{\lim}\left(\tilde{\Omega}\right) + n_b \sigma$$

It is convenient to model the interface between a solid electrolyte and solid electrode in the slab geometry using a periodic simulation cell:

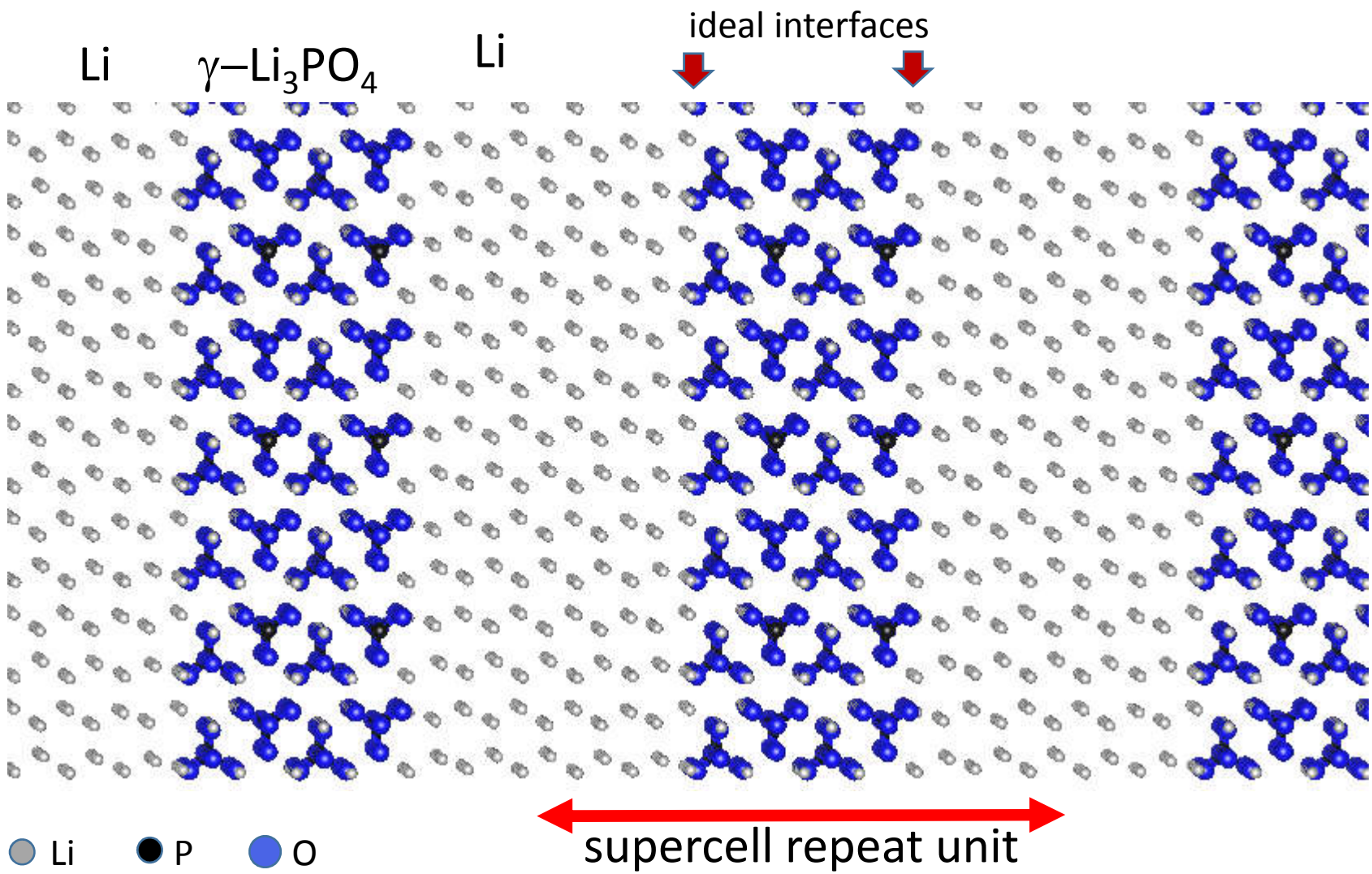

Lepley's linear equation for the interface energy: $\tilde{\gamma}_{ab}\left(\tilde{\Omega}, n_a, n_b\right) = \tilde{\gamma}_{ab}^{\lim}\left(\tilde{\Omega}\right) + n_b\sigma$

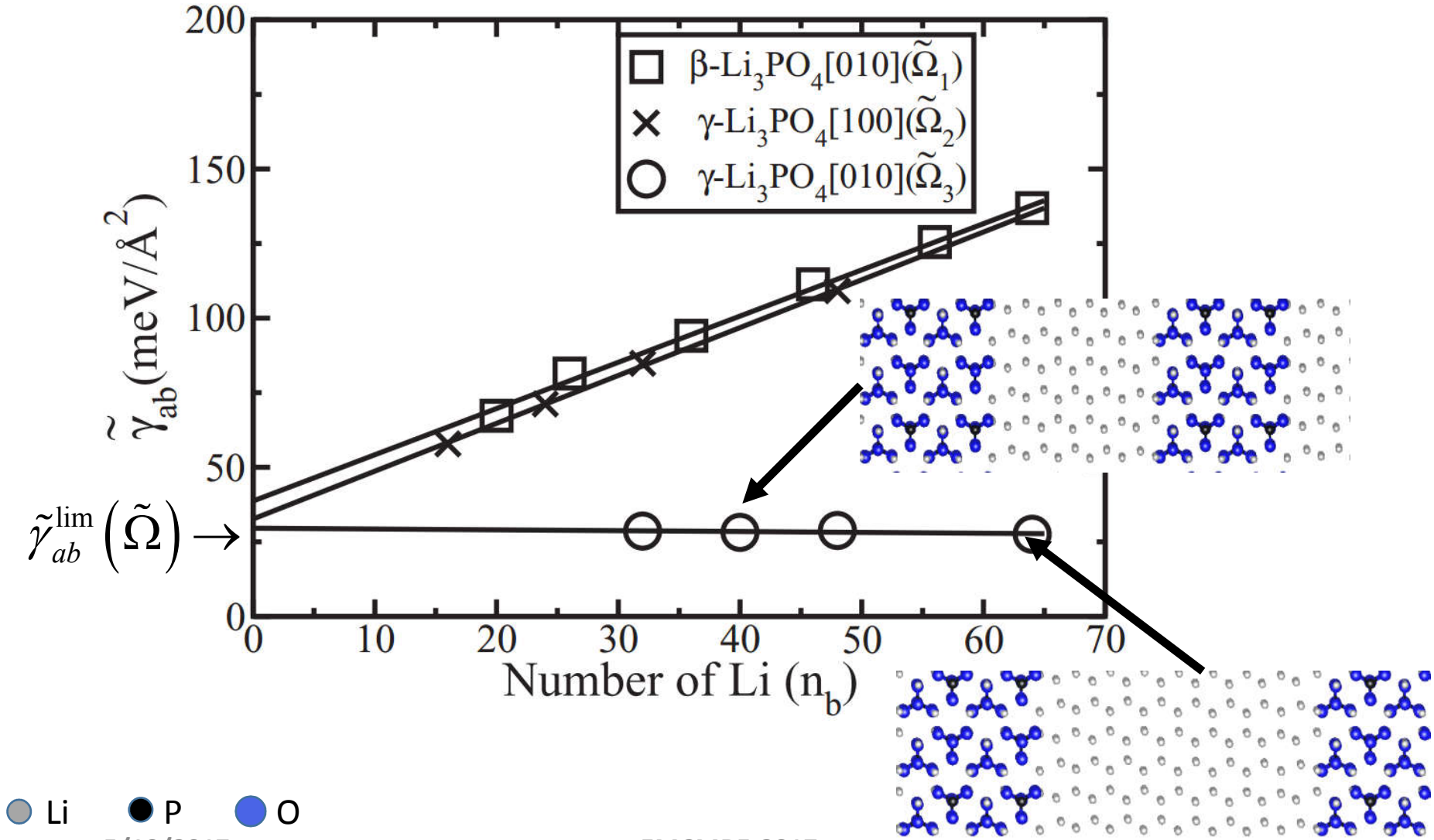

Energy diagram for ideal electrolyte/metal interface

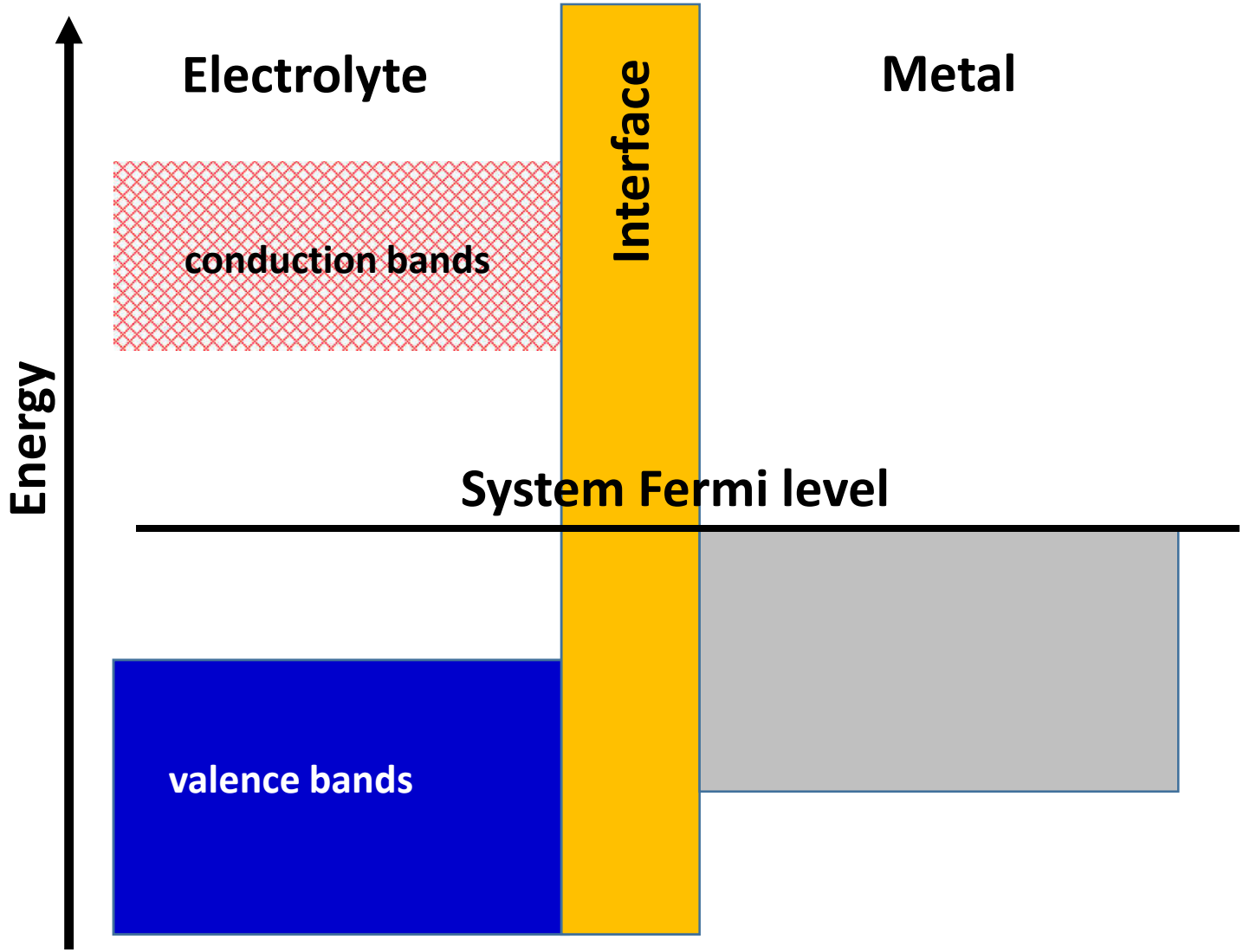

$Li_{14}P_2O_3N_6$ interfaced with Li metal
Al-Qawasmeh and Holzwarth, to be published

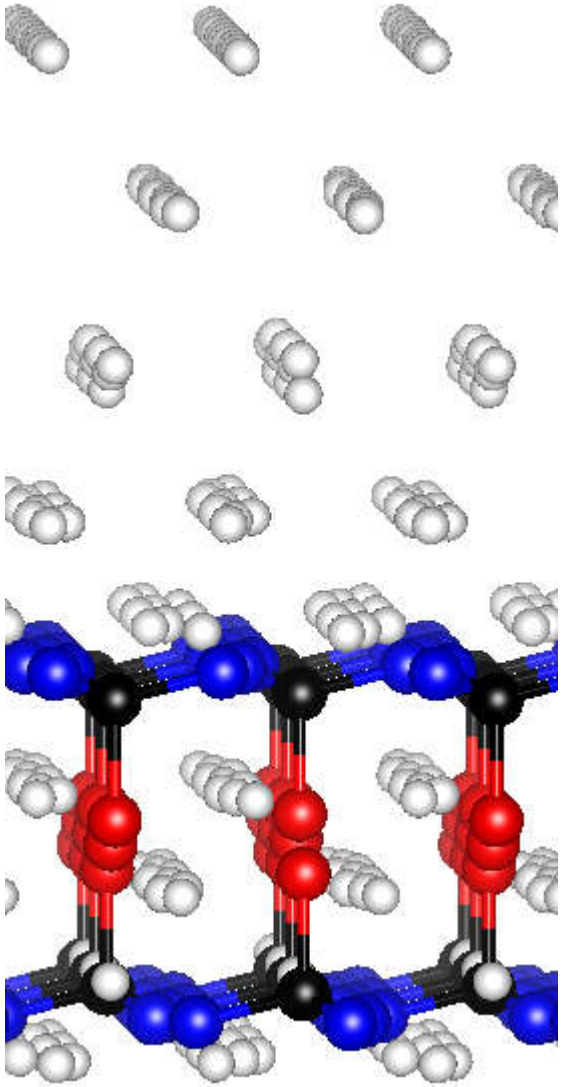

Partial densities of states plots

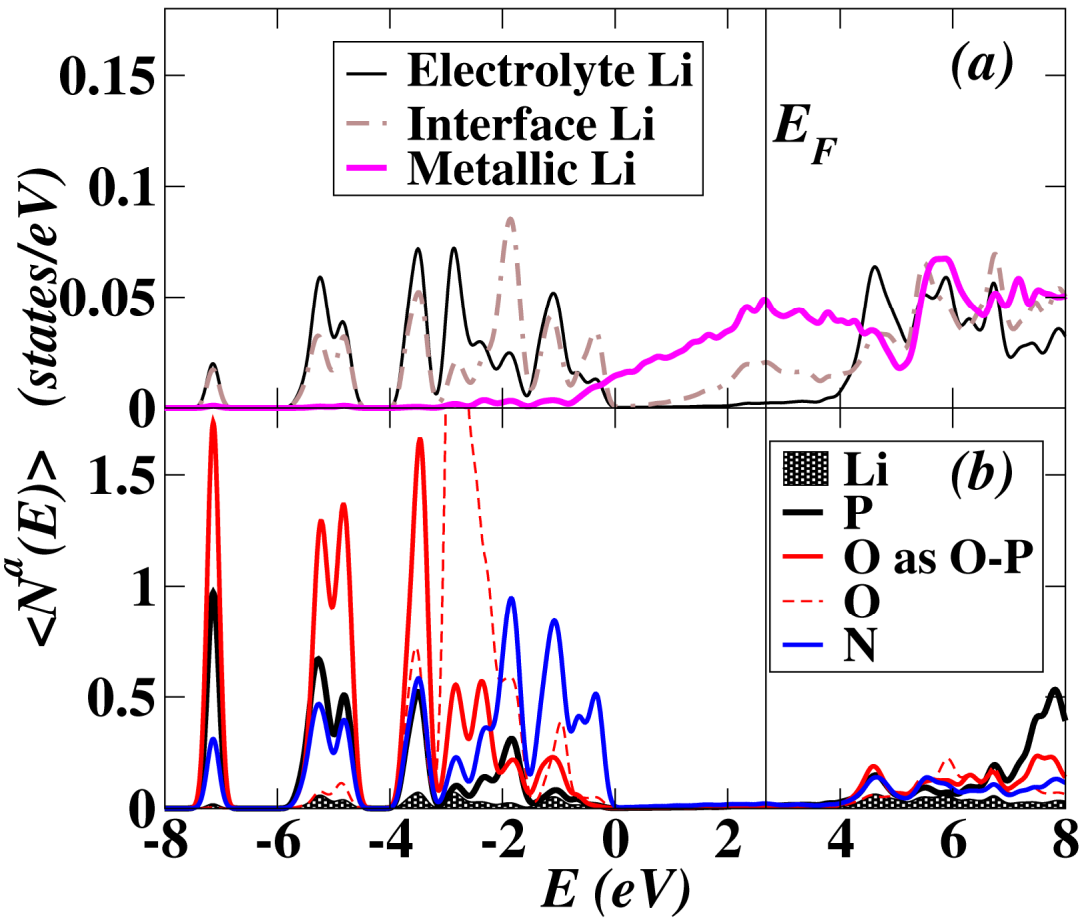

γ–Li_3PS_4 [010]/Li_2S [110]

Li P S

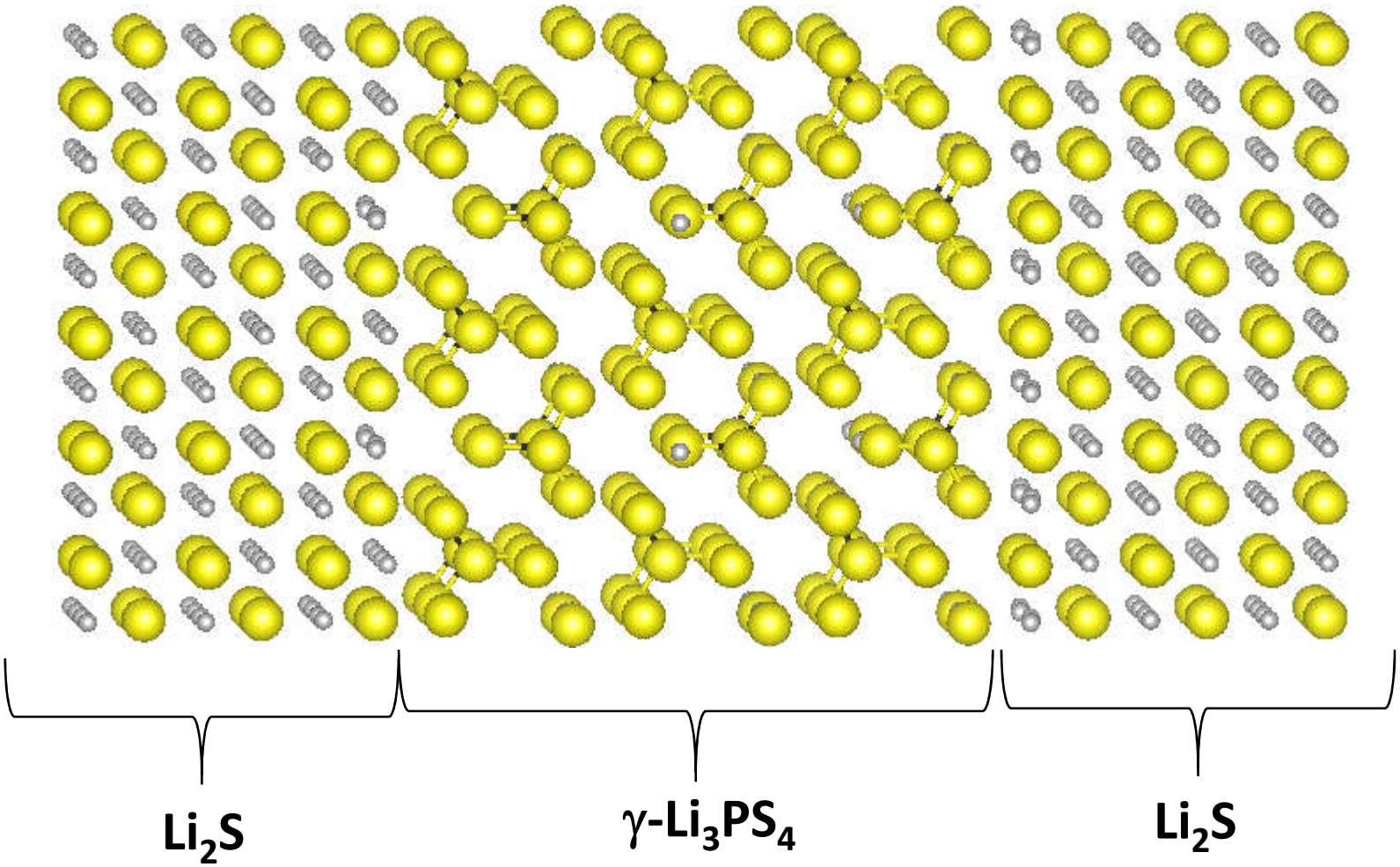

Stable interface; composite electrolyte system

γ–Li_3PS_4 [010]/Li

Li P S

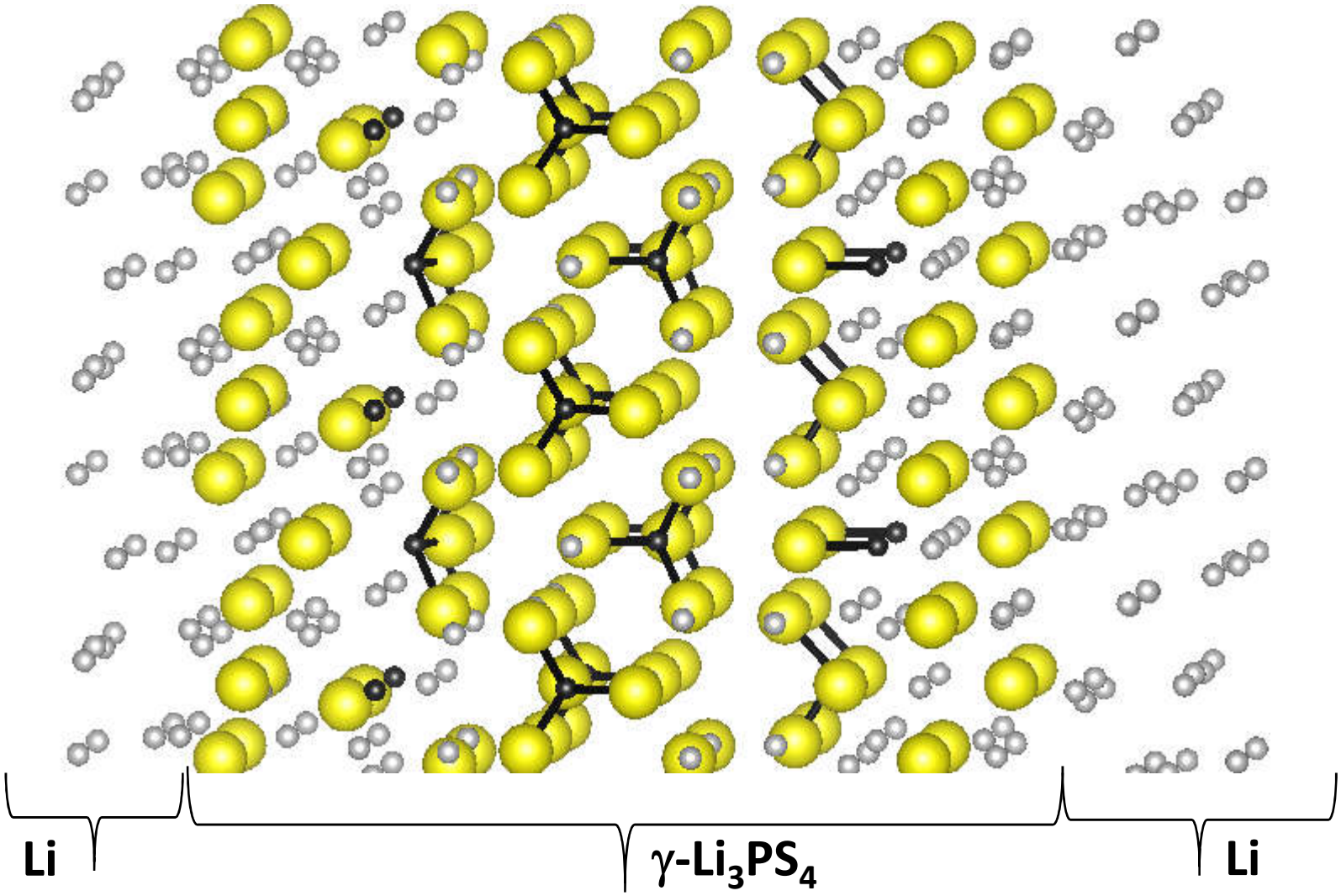

Initially unstable interface; (meta)-stable buffer layer formed

Partial density of states analysis of unstable Li_3PS_4/Li interface:

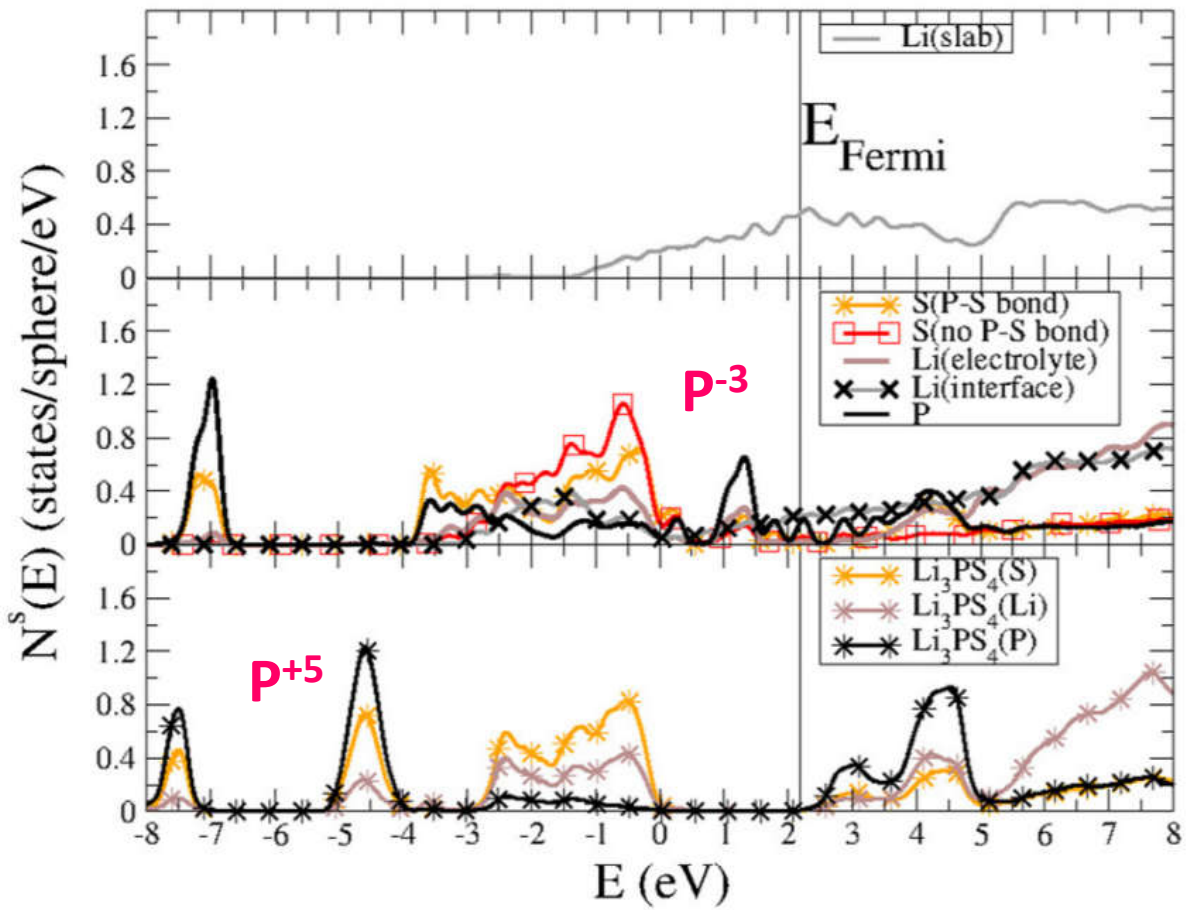

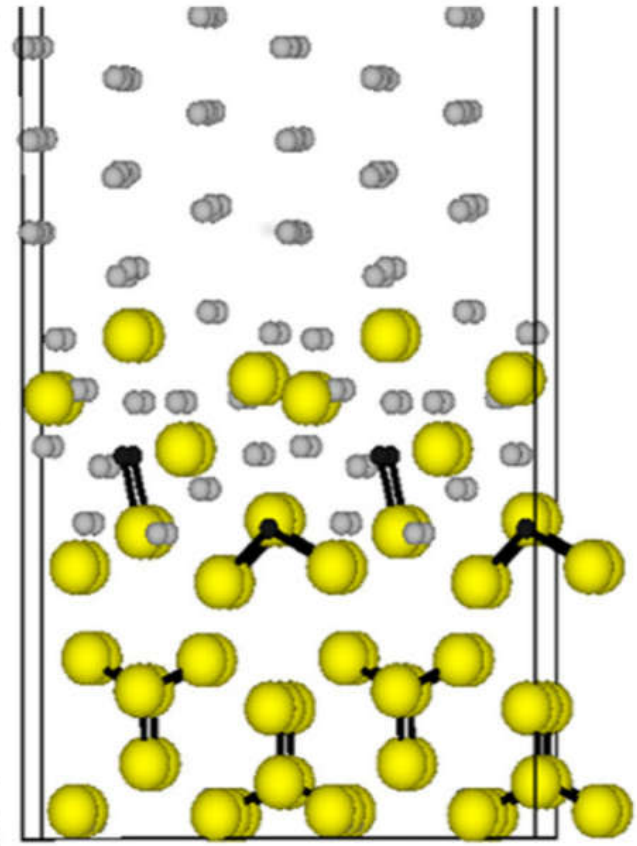

$$Li_3PS_4 + 8Li \longrightarrow Li_3P + 4Li_2S + 12.30\ eV$$

Bulk reactions from estimated heats of formation

$$Li_3PS_4 + 8Li \longrightarrow Li_3P + 4Li_2S + 12.30\ eV$$

Decomposition at interface

$$Li_3PO_4 + 8Li \longrightarrow Li_3P + 4Li_2O + 6.64\ eV$$

(Meta-)stable interface

Evidence of kinetic barrier at Li_3PO_4/Li interface

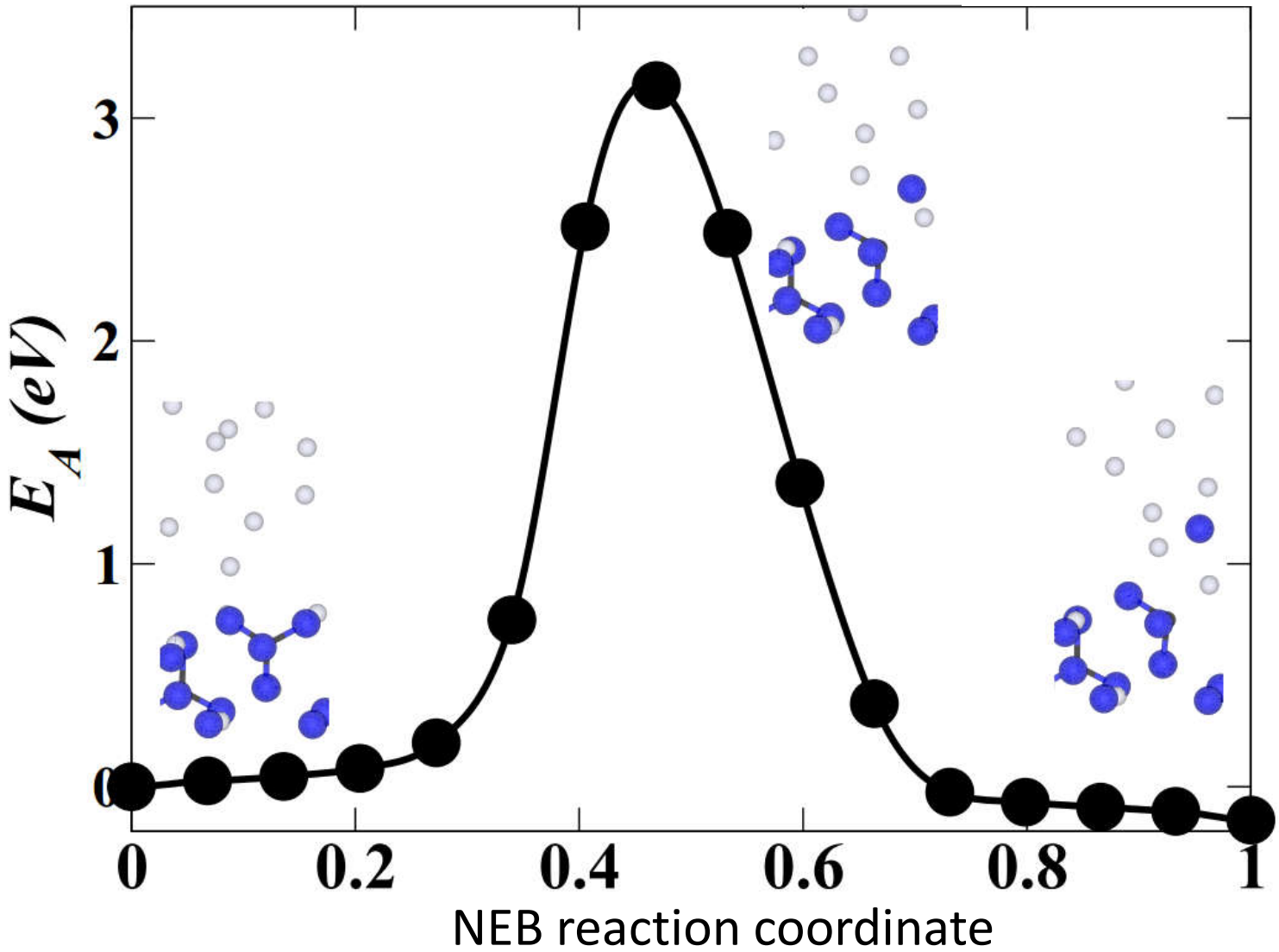

WAKE FOREST UNIVERSITY

Summary of ideal interface story

- A practical scheme was developed to compute an intensive measure of the interface interaction $\tilde{\gamma}_{ab}^{\text{int}}$, explicitly accounting for the effects of lattice stain.
- Discussed bulk reactivity as related to the interface stability of the interfaces of
  - Li_3PO_4/Li (having a significant kinetic barrier to decomposition)
  - Li_3PS_4/Li (having localized decomposition).

Additional thoughts

- Limitations of first principles modeling
  - Small simulation cells
  - Zero temperature
- Possible extensions
  - Develop approximation schemes for treatment of larger supercells
  - Use molecular dynamics and/or Monte Carlo techniques
- Ideal research effort in materials includes close collaboration of both simulations and experimental measurements.
- For battery technology, there remain many opportunities for new materials development.